

Adaptive Bit Allocation With Reduced Feedback for Wireless Multicarrier Transceivers

Udaya Kiran Tadikonda

Bachelor of Technology
Electronics & Communications Engineering
Jawaharlal Nehru Technological University, India, 2005

Submitted to the Department of Electrical Engineering &
Computer Science and the Faculty of the Graduate School
of the University of Kansas in partial fulfillment of
the requirements for the degree of Master of Science

Thesis Committee:

Dr. Glenn E. Prescott: Chairperson

Dr. Alexander M. Wyglinski: Co-Chair

Dr. Gary J. Minden

Dr. Joseph B. Evans

Date Defended: 12/07/2007

The Thesis Committee for Udaya Kiran Tadikonda certifies
that this is the approved version of the following thesis:

**Adaptive Bit Allocation With Reduced Feedback for Wireless
Multicarrier Transceivers**

Committee:

Chairperson

Co-Chair

Date Approved

Abstract

With the increasing demand in the wireless mobile applications came a growing need to transmit information quickly and accurately, while consuming more and more bandwidth. To address this need, communication engineers started employing multicarrier modulation in their designs, which is suitable for high data rate transmission. Multicarrier modulation reduces the system's susceptibility to the frequency-selective fading channel, by transforming it into a collection of approximately flat subchannels. As a result, this makes it easier to compensate for the distortion introduced by the channel. This thesis concentrates on techniques for saving bandwidth usage when employing adaptive multicarrier modulation, where subcarrier parameters (bit and energy allocations) are modulated based on the channel state information feedback obtained from previous burst.

Although bit and energy allocations can substantially increase error robustness and throughput of the system, the feedback information required at both ends of the transceiver can be large. The objective of this work is to compare different feedback compression techniques that could reduce the amount of feedback information required to perform adaptive bit and energy allocation in multicarrier transceivers.

This thesis employs an approach for reducing the number of feedback transmissions by exploiting the time-correlation properties of a wireless channel and placing a threshold check on bit error rate (BER) values. Using quantization and source coding techniques, such as Huffman coding, Run length encoding and LZW algorithms, the amount of feedback information has been compressed. These calculations have been done for different quantization levels to understand the relationship between quantization levels and system performance. These techniques have been applied to both OFDM and MIMO-OFDM systems.

To my parents and my sister

Acknowledgements

I would like to express my deep gratitude to my advisor, Dr. Alexander M. Wyglinski, for all the endless hours of help, suggestions, ideas and advice during the development of this thesis. I would like to thank him for the continuous support and cooperation. It has been a great experience working with him as a part of the Signals Modulation and Routing (SMART) group at ITTC, KU. I would like to also thank Dr. Glenn Prescott for serving as the chairperson during the final semester of my study.

I would like to thank my committee members, Dr. Gary J. Minden and Dr. Joseph B. Evans, for serving on my committee and offering valuable advice and input during my research. I would like to specially thank Dr. Fabrice Labeau, McGill University, Canada, for all the invaluable hours spent on telephone conversations providing me with great suggestions and help whenever required.

I would like to thank all my friends here at KU who have made my study a great experience. I would like to mention SMART group members, Moses, Madhu, Mithun, Pramodini, and especially Priyanka, who have shown constant support and love.

I am deeply grateful to my parents and sister for their strong support and encouragement for pursuing this Master's degree. Special thanks to my sister who has been a great inspiration to me.

Contents

Acceptance Page	i
Abstract	ii
Acknowledgements	iv
1 Introduction	1
1.1 Motivation	1
1.2 Research Objective	4
1.3 Contributions	5
1.4 Thesis Outline	6
2 Background	8
2.1 OFDM Framework	8
2.1.1 Introduction to OFDM	8
2.2 MIMO-OFDM	22
2.3 Channel Model	25
2.3.1 Time-Varying Channel Correlation Models	29
2.4 Quantization	33
2.5 Data Compression Techniques	36
2.5.1 Huffman Coding	37
2.5.2 Run Length Encoding (RLE)	39
2.5.3 LZW Compression	41
2.6 Chapter Summary	44
3 Feedback in Adaptive OFDM and MIMO-OFDM Systems	46
3.1 Feedback Data Analysis	46

3.1.1	Adaptive Bit Allocation	46
3.2	Related Research	57
3.3	Chapter Summary	59
4	Feedback Compression in Adaptive OFDM and MIMO-OFDM Systems	60
4.1	Feedback Reduction Scheme	60
4.2	Simulation Results and Comparison	67
4.2.1	Simulation Parameters	67
4.2.2	Results	70
4.3	Chapter Summary	89
5	Conclusions	91
5.1	Future Work	93
	References	94

List of Figures

2.1	Frequency Response of a Single Carrier, Multicarrier and Frequency-selective Fading Channel	10
2.2	Basis Functions of OFDM system	11
2.3	Illustration of FDM and OFDM Spectrum Occupancy	11
2.4	Block Diagram of an Adaptive OFDM System Describing the Feedback of Allocation Parameters.	12
2.5	Cyclic Prefix Illustration in OFDM Symbol	14
2.6	Example Showing Bit Allocations by a Bit Loading Algorithm	16
2.7	MIMO System With T Transmit Antennas and R Receive Antennas.	23
2.8	A Schematic Illustration of Channel Model. (a) Exponentially Decaying Ray and Cluster Average Powers. (b) Channel Impulse Response (from [28]).	29
2.9	Uncorrelated Time-varying Channel Model	31
2.10	99% Correlated Time-varying Channel Model	31
2.11	95% Correlated Time-varying Channel Model	32
2.12	85% Correlated Time-varying Channel Model	32
2.13	Uniform and Nonuniform Quantizers	35
2.14	Huffman Coding Example	38
2.15	RLE Coding Example	40
2.16	Illustration of LZW Compression	42
3.1	Different Subcarriers BER Performance Illustration	47
3.2	MCM Transmitter and Receiver With Adaptive Bit Loading Algorithm	51
3.3	Chow's Bit Loading Algorithm	53

3.4	Flowchart Describing the Campello's Optimization Algorithm of Bit Allocation	54
3.5	Algorithm to Deal With Single Violated Bit Constraint	56
3.6	Energy and Bit Allocation for a Channel Instance	56
4.1	General OFDM Schematic Employing Feedback Reduction Scheme	61
4.2	Description of the Feedback Reduction Scheme for Feedback Transmission Reduction in Adaptive Multicarrier Systems With Channel Correlations varying from 1% to 99%.	63
4.3	Description of Feedback Data Compression Methods Employed to Compress the Reduced Feedback Data in Adaptive Multicarrier Systems With Channel Correlations varying from 1% to 99%. . .	65
4.4	Feedback Size Ratio of a Normal OFDM and MIMO-OFDM Systems for Different Channel Correlations. Total Transmitted Bits = 5120000.	68
4.5	BER of Individual Channel Instances of an OFDM System for 99% Correlated Channel at SNR=15dB.	71
4.6	BER of Individual Channel Instances of a MIMO 2x2 System for 99% Correlated Channel at SNR=15dB.	72
4.7	BER of Individual Channel Instances of a MIMO 4x4 System for 99% Correlated Channel at SNR=15dB.	72
4.8	Reduction in Number of Feedback Transmissions Achieved Using Feedback Reduction Scheme in OFDM and MIMO-OFDM Systems.	73
4.9	Average BER Value Curves of OFDM and MIMO-OFDM Systems for Various Channel Correlations.	75
4.10	Reduction in Feedback Size Ratio Achieved Using the Feedback Reduction Scheme in OFDM and MIMO-OFDM Systems. Solid Lines for Reduced Feedback and Dotted Lines for Unreduced Feedback. Total Transmitted Bits = 5120000.	76
4.11	Compression of Feedback Size Ratio Achieved in OFDM and MIMO-OFDM Systems Using Run Length Coding. Solid Lines for Compressed Feedback and Dotted Lines for Unreduced Feedback. Total Transmitted Bits = 5120000.	78

4.12	Compression of Feedback Size Ratio Achieved in OFDM and MIMO-OFDM Systems Using Huffman Coding. Solid Lines for Compressed Feedback and Dotted Lines for Unreduced Feedback. Total Transmitted Bits = 5120000.	79
4.13	Compression of Feedback Size Ratio Achieved in OFDM and MIMO-OFDM Systems Using LZW Coding. Solid Lines for Compressed Feedback and Dotted Lines for Unreduced Feedback. Total Transmitted Bits = 5120000.	81
4.14	Mean of Average BER Curves for Various Energy Allocation Quantization Levels in OFDM and MIMO-OFDM Systems.	83
4.15	Reduction in Feedback Size Ratios Achieved Using Feedback Reduction Scheme for Various Energy Allocation Quantization Levels in OFDM and MIMO-OFDM Systems.	85
4.16	Compressed Feedback Size (RLE) Ratios for Various Energy Allocation Quantization Levels in OFDM and MIMO-OFDM Systems.	86
4.17	Compressed Feedback Size (Huffman) Ratios for Various Energy Allocation Quantization Levels in OFDM and MIMO-OFDM Systems.	87
4.18	Compressed Feedback Size (LZW) Ratios for Various Energy Allocation Quantization Levels in OFDM and MIMO-OFDM Systems.	88

Chapter 1

Introduction

1.1 Motivation

Although in use for many years, multi-carrier modulation (MCM) has recently become an attractive technique to many digital communication systems. The main idea of an MCM system is to split a high-rate data stream into several slow-rate data sequences, and to use these to modulate a set of parallel subchannels that makes full use of the available bandwidth. When the channel introduces inter-symbol interference (ISI), a system using MCM does not need a complex equalizer at the receiver end. This is a useful property when dealing with time-dispersive channels and high data rates.

From a time-domain perspective, this translates the wideband transmission system into a collection of parallel narrowband transmission systems, each operating at a lower data rate. From the frequency-domain perspective, MCM transforms the frequency-selective channel, i.e., non-flat spectrum across the frequency band of interest, into a collection of approximately flat subchannels over which the data gets transmitted in parallel. Thus, MCM has become one of the choices

to combat frequency-selective fading channel.

Orthogonal frequency division multiplexing (OFDM) [1] is one of the most popular types of MCM schemes. It is an enhanced extension of frequency division multiplexing (FDM), where the parallel subchannels have overlapped spectra. Nevertheless, due to their orthogonality, data can be recovered at the receiver without interference from adjacent subcarriers. As a direct consequence, these systems have high spectral efficiency. This is another prominent feature that modern digital transceivers demand, as it leads to less interference (unlike GSM channels which overlap but are not orthogonal, and thus interfere with each other to some extent [2]).

Over the past several years, OFDM has received considerable attention from the general wireless community, in particular from the wireless LAN (WLAN) standards groups, because of its capability to exploit wideband multipath conditions. Digital terrestrial television broadcast (DTTB) standards specified the use of OFDM modulation in Europe (ETSI DVB-T) and Japan (ARIB ISDB-T). Similarly, wireless local area network (WLAN) standards, also specifying OFDM modulation, are currently being finalized in Europe (ETSI HIPERLAN/2), North America (IEEE 802.11a) and Japan (ARIB HiSWANa). OFDM was also one of the candidate transmission techniques for UMTS and is now proposed for IEEE 802.16a and ETSI BRAN HIPERMAN for broadband wireless access networks. The success of OFDM in recent wired and wireless broadband communications systems strongly suggests that it could be a leading candidate for a future cellular communications standard, i.e. 4G.

However, many of these MCM systems, especially the wireless ones [3], use conventional multicarrier modulation techniques, which employ the same signal

constellation across all the subcarriers. As a result, these systems suffer from the subcarriers with poor error performance. For example, it is possible that a given subchannel has a low gain, resulting in a large BER. Adaptive modulation is an important technique that has been known to yield increased data rates for high-speed wireless data transmission when OFDM is employed. However, accurate channel state information (CSI) is required at both transmitter and receiver to achieve the benefits. Given this knowledge, both the transmitter and receiver can have an agreed-upon modulation scheme for increased performance. This modulation scheme might be different for different subcarriers. As a part of the feedback, either bit and energy allocations to be used for next transmissions or signal to noise ratio (SNR) values of each subcarrier are sent. The bit allocations define the modulation scheme to be used, and the energy allocations define the extra energy required to transmit the new number of bits assigned on the subcarrier. Since the modulation parameters are set according to the channel conditions, we do not waste resources (power, or complex channel coding) when the channel is known to be bad. And analogously we can benefit from a good channel by using, for instance, higher order constellations to increase the data rate while keeping the average transmitted power nearly constant.

In this thesis, we consider adaptive bit and power allocation schemes. Namely, we presuppose a desired number of bits to be transmitted by a single OFDM symbol (consisting of N subcarriers), and we load these bits onto the subcarriers in such a way that minimum energy is allocated to the entire transmission. A number of loading algorithms [4] have been developed and implemented by various researchers.

OFDM may be combined with antenna arrays at the transmitter and receiver

to increase the diversity gain and/or to enhance the system capacity on time-varying and frequency-selective channels, resulting in a multiple-input multiple-output (MIMO) configuration [5]. MIMO refers to the use of multiple antennas both at the transmitter and receiver to improve the performance of communication systems. A MIMO system takes advantage of the spatial diversity that is obtained by spatially separated antennas in a dense multipath scattering environment. A key concept employed here is that every matrix channel can be decomposed into a set of parallel subchannels over which data can be transmitted independently, given appropriate precoding and shaping transformations at the transmitter and receiver, respectively.

This thesis concentrates on comparing different compression techniques when employed along with the scheme used for reduction of the number of feedback transmissions in adaptive OFDM and MIMO-OFDM systems.

1.2 Research Objective

Much research has been done on the performance of adaptive multicarrier systems. Some researchers assumed perfect channel knowledge [6–9], but they were overly optimistic. They assumed ideal conditions and so, their results in terms of performance were very good, which may or may not be correct when applied to the actual situation. Others attempted to provide more accurate results by considering the sources of uncertainty [10, 11] and outdated channel estimates [11, 12]

As the number of subcarriers increase to provide better data rates in the adaptive systems, the amount of feedback increases, as the feedback data is directly proportional to number of subcarriers. Thus, feedback occupies more bandwidth

reducing system throughput. Some of the research was also aimed at the overhead information and its compression [13, 14]. However, less research has been done on the feedback data and its bandwidth occupancy, which has to be sent to the transmitter for making the system adaptive. The feedback information size is directly proportional to the number of subcarriers N . For example, for each channel instance there would be N number of bits and energy values. Converting them to binary bits before transmission will increase the size the feedback data basing on the number of bits used to represent the allocations. The large amount of CSI feedback and signaling transmissions will be a serious problem in adaptive OFDM and MIMO-OFDM systems.

The primary goal of this thesis is to compress the feedback data using various lossless compression algorithms along with a feedback reduction scheme. We also hope to develop a thorough understanding of how the quality of feedback information affects the performance of a multicarrier transceiver employing adaptive loading algorithms by employing various quantization levels in the simulation.

1.3 Contributions

This thesis presents the following approach to compress the feedback data:

Since the wireless channel is a time-varying channel and there can be any amount of channel correlation present, a feedback reduction scheme has been used in this thesis which exploits the time-correlation properties of the wireless channel and based on the BER performance of the system, decides if the system needs newer allocation parameters or can continue with old allocations. This is done by using a threshold check on BER values and by allowing feedback consisting of bit and energy allocations to be transmitted only when the threshold check

is positive. With the help of this scheme, a reasonable reduction in the number of feedback transmissions has been achieved which varies for different time-varying correlated channels. Since the main motivation of this thesis is to compress the feedback data, various suitable lossless compression algorithms have been considered, such as Huffman coding, Run length encoding and Lempel-Ziv-Welch (LZW) compression. Since we have the advantage of having reduced feedback data even before applying these compression techniques, a significant compression has been achieved. Huffman coding dominated two other compression algorithms by achieving higher compression ratios in worst channel correlation conditions. Also, the system performance has been tested for various quantization levels and a thorough understanding between the number of quantization levels and compression ratios has been achieved. The main contribution of this thesis starts with being able to reduce the number of feedback transmissions by taking advantage of the time-correlation properties of a wireless channel, using the feedback reduction scheme. Achieved significant compression ratios by applying lossless compression algorithms on the feedback data and compared their performance for different quantization levels and channel conditions. An understanding on the varying quality of feedback data and its effect on the system performance has been analyzed.

1.4 Thesis Outline

This thesis is organized as follows: Chapter 2 consists of a review of the main aspects of MCM, OFDM and the channel decomposition method of MIMO-OFDM, that will be needed in subsequent sections. A brief description of the time-varying channels of different correlations, quantization methods and source

coding techniques which are employed in this work are given.

Chapter 3 deals with the energy and bit allocations across the OFDM and MIMO-OFDM subcarriers. Special attention will be placed on adaptive modulation techniques and the analysis of algorithms used for optimal bit-loading strategy. A brief summary of various approaches is also given.

In Chapter 4, the feedback data reduction scheme is explained in detail and simulation results obtained by using this scheme along with different compression algorithms are presented. A detailed discussion about the results obtained is also provided.

Finally, in Chapter 5, several conclusions are drawn and directions for future research is presented.

Chapter 2

Background

2.1 OFDM Framework

This section discusses the evolution of OFDM starting, from single carrier transmission, and then frequency division multiplexing leading to OFDM and MIMO. A brief description of other key system aspects, feedback channels and their estimation, time-varying channel correlation models, quantization methods, and data compression techniques is given.

2.1.1 Introduction to OFDM

Single Carrier Transmission

A single carrier system modulates information onto one carrier (usually a sinusoidal waveform) using the frequency, phase, or amplitude adjustment of the carrier. For digital signals, information is in the form of bits, or collections of bits mapped to symbols, that are modulated onto a carrier. In telecommunications, bit rate or data rate (represented as R or f_b) is the number of bits transmitted over a communication link per unit of time. We know that $f = 1/t$, so for higher

bandwidths (data rates, f), the duration of one bit or symbol of information (t) becomes smaller. As a result the system becomes more susceptible to the loss of information from impulse noise, signal reflections, and other impairments. These impairments can impede the ability of the communication system to recover the transmitted information. In addition, as the bandwidth used by a single carrier system increases, the susceptibility to interference from other signal sources becomes greater. This type of interference is commonly labeled as carrier wave (CW) or frequency interference.

Frequency Division Multiplexing (FDM)

Frequency division multiplexing (FDM) extends the concept of single carrier modulation by using multiple subcarriers within the same single transmission channel. FDM divides the channel bandwidth into subchannels and transmits multiple relatively low data rate signals by carrying each signal on a separate carrier frequency. Data transmitted using FDM do not have to be divided evenly, nor do they have to originate from the same information source. Advantages of FDM include using separate modulation/demodulation schemes customized to a particular type of data, or sending out banks of dissimilar data that can be best sent using multiple, and possibly different, modulation schemes.

FDM offers an advantage over single-carrier modulation in terms of narrow-band frequency interference since this interference will only affect one of the frequency subbands. The other subcarriers will not be affected by the interference. Since each subcarrier has a lower information rate, the data symbol periods in a digital system will be longer, adding some additional immunity to impulse noise and reflections. To ensure that the signal of one subchannel does not overlap with the signal from an adjacent one, in an FDM transmission, guard-bands are used

between the subchannels which leads to effective usage of spectrum.

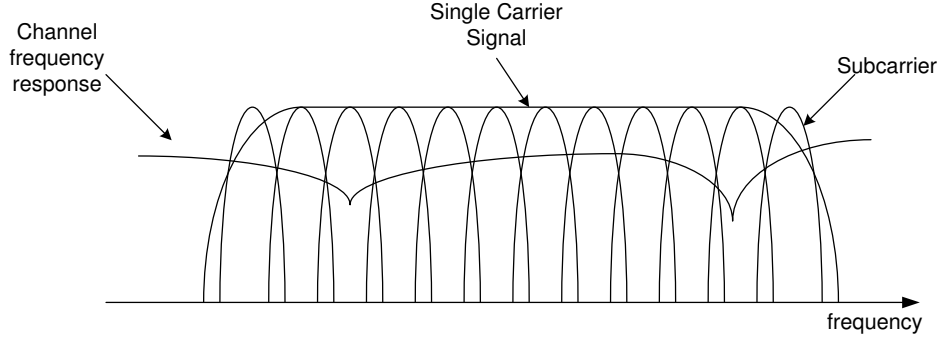


Figure 2.1. Frequency Response of a Single Carrier, Multicarrier and Frequency-selective Fading Channel

Orthogonal Frequency Division Multiplexing (OFDM)

Figure 2.1 shows the frequency response of a single carrier transmission and multicarrier transmission over a frequency-selective fading channel. Single carrier system suffers information loss when the channel fading is deep, whereas multicarrier transmission experiences a flat fading in all its subcarriers and very less information loss. In order to solve the bandwidth efficiency problem, orthogonal frequency division multiplexing (OFDM) was proposed, where the different carriers are orthogonal to each other, allowing for overlapping subchannels in the frequency domain. The basis functions of an OFDM system are represented in Figure 2.2. As shown in Figure 2.3, we can see that for a given bandwidth the number of subcarriers OFDM can employ are almost double the subcarriers of FDM, which explains the bandwidth saving of OFDM over FDM. This carrier spacing provides optimal spectral efficiency. In OFDM systems, because of the overlapping subcarriers, spectrum is efficiently utilized. But in FDM, as there is a need for usage of guard-bands, some of the spectrum is wasted. Today OFDM has become a very popular choice of transmission technology.

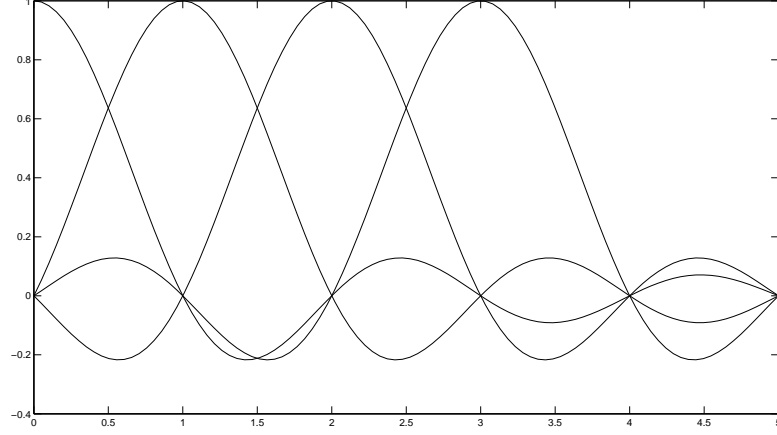


Figure 2.2. Basis Functions of OFDM system

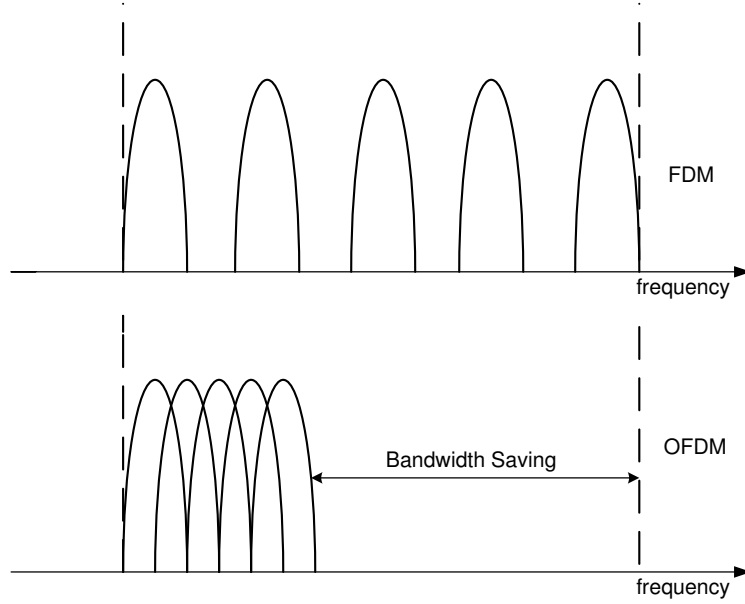


Figure 2.3. Illustration of FDM and OFDM Spectrum Occupancy

The OFDM system studied in this thesis has the block structure as shown in Figure 2.4 [15]. The system determines the constellation scheme of each sub-carrier and then maps the input bits into complex-valued symbols $X(n)$ in the modulation block. The number of bits per symbol assigned to each subcarrier,

which is based on the signal to noise ratio of each subcarrier in the frequency range, is determined using an adaptive bit loading algorithm, which will be detailed in the next chapter. In practice, OFDM systems are implemented using a combination of fast fourier transform (FFT) and inverse fast fourier transform (IFFT) blocks that are mathematically equivalent versions of the discrete fourier transform (DFT) and inverse discrete fourier transform (IDFT), respectively. The IFFT block modulates $X(n)$ onto N orthogonal subcarriers which is actually converting the system into time domain from frequency domain. A cyclic prefix is then added to the multiplexed output of the IFFT block. The output signal is then converted into a continuous time analog signal before it is transmitted through the wireless channel. At the receiver side, an inverse operation is carried out and the information data are detected.

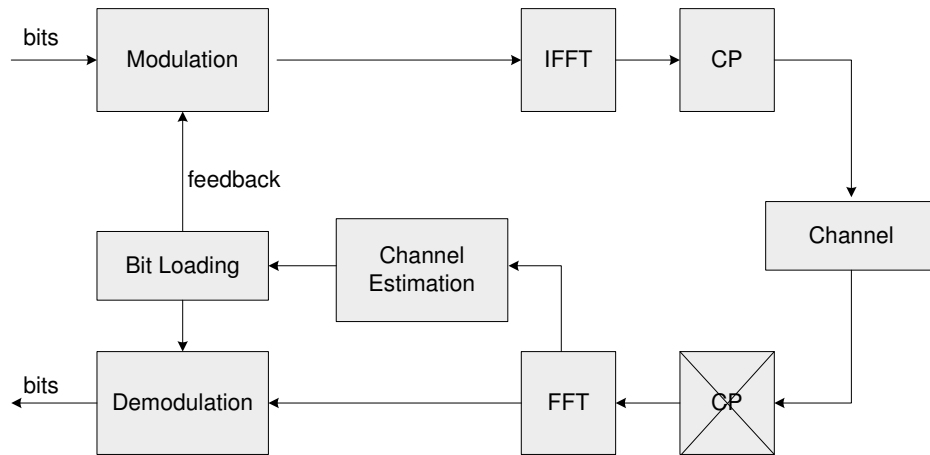


Figure 2.4. Block Diagram of an Adaptive OFDM System Describing the Feedback of Allocation Parameters.

2.1.1.1 FFT and IFFT

The key components of an OFDM system are the IFFT at the transmitter and FFT at the receiver. These operations perform linear mappings between N

complex data symbols and N complex OFDM symbols. The reason for these operations is to transform the high data rate stream into N low data rate streams with each experiencing a flat fading portion of the channel during the transmission. Suppose the data set to be transmitted is $X(1), X(2), \dots, X(N)$, where N is the total number of subcarriers. The discrete-time representation of the signal after IFFT is [16]:

$$x(n) = \frac{1}{\sqrt{N}} \sum_{k=0}^{N-1} X(k) e^{j2\pi k \frac{n}{N}}, \quad n = 0 \dots N-1. \quad (2.1)$$

At the receiver side, the data are recovered by performing FFT on the received signal [16]:

$$Y(k) = \frac{1}{\sqrt{N}} \sum_{n=0}^{N-1} x(n) e^{-j2\pi k \frac{n}{N}}, \quad k = 0 \dots N-1. \quad (2.2)$$

An N -point FFT only requires $N \log(N)$ multiplications.

2.1.1.2 Cyclic Prefix

Two difficulties arise when the OFDM signal is transmitted over a dispersive channel. One difficulty is that channel dispersion destroys the orthogonality between subcarriers and causes intercarrier interference (ICI). In addition, a system may transmit multiple OFDM symbols in a series so that a dispersive channel causes intersymbol interference (ISI) between successive OFDM symbols. The insertion of a silent guard period between successive OFDM symbols would avoid ISI in a dispersive environment, but it does not avoid the loss of the subcarrier orthogonality [17]. This problem is solved with the introduction of a cyclic prefix.

The cyclic prefix is a crucial feature of OFDM which combats the effects of multipath. ISI and ICI are avoided by introducing a guard interval at the front, which is appending a copy of the last part of the OFDM symbol at the front of

the transmitted symbol. The cyclic prefix still occupies the same time interval as guard period, but it ensures that the delayed replicas of the OFDM symbols will always have a complete symbol within the FFT interval (often referred as FFT window); this makes the transmitted signal periodic. This periodicity plays a very significant role, as this helps maintaining orthogonality. Figure 2.5 illustrates the idea.

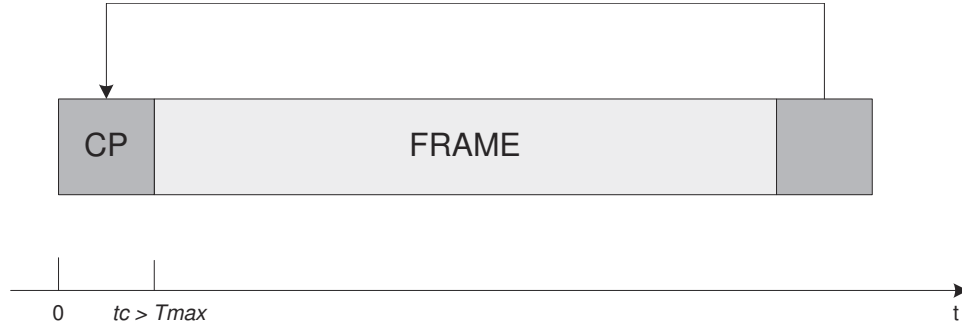


Figure 2.5. Cyclic Prefix Illustration in OFDM Symbol

The idea is to convert the linear convolution (between signal and channel response) into a circular convolution. In this way, the FFT of the circular convolution of two signals is equivalent to the multiplication of these signals in the frequency domain. However, in order to preserve the orthogonality property, T_{max} should not exceed the duration of the time guard interval. As shown in Figure 2.5, once the above condition is satisfied, there is no ISI since the previous symbol will only have effect over samples within $[0, T_{max}]$. It is clear that orthogonality is maintained so that there is no ICI. Another advantage with the cyclic prefix is that it serves as a guard interval between consecutive OFDM frames. This is similar to adding guard bits, which means that the problem with inter-frame interference also will disappear. To conclude, the cyclic prefix gives a two-fold advantage, first occupying the guard interval, it removes the effect of ISI, and by

maintaining orthogonality it completely removes the ICI. This often motivates the use of OFDM in wireless systems.

2.1.1.3 Modulation and Demodulation

A modulator maps a set of bits into a complex number corresponding to an element of a signal constellation. Given an adaptive algorithm, the modulator has an input of a set of bits and energy values. The output of the modulator is a constellation symbol corresponding to the number of bits on the input, appropriately scaled to have a desired energy level.

The modulator is chosen to have a finite number of rates available, which means that only a finite number of constellations are available for modulation. Only six different square M-order quadrature amplitude modulation (MQAM) signal constellations are used; this scheme is expected to perform with an efficiency very close to that resulting from using unrestricted constellations [18]. The modulator maps either 1 bit, 2 bits, 4 bits, 6 bits, or 8 bits into a symbol, which means that it can perform only binary phase shift keying (BPSK), quadrature phase shift keying (QPSK), 16 quadrature amplitude modulation (16QAM), 64 quadrature amplitude modulation (64QAM), and 256 quadrature amplitude modulation (256QAM) modulation on each subcarrier. Further, in order to provide robustness against bit errors, gray-coded constellations are employed for each modulation order available. This Gray coding ensures that if a symbol error occurs, where the decoder selects an adjacent symbol to that which the transmitter intended to be decoded, there is only a single bit error resulting. Shown in Figure 2.6 are the bit allocations being provided by a bit loading algorithm to the transmitter.

Demodulation is performed using a maximum likelihood (ML) approach, given

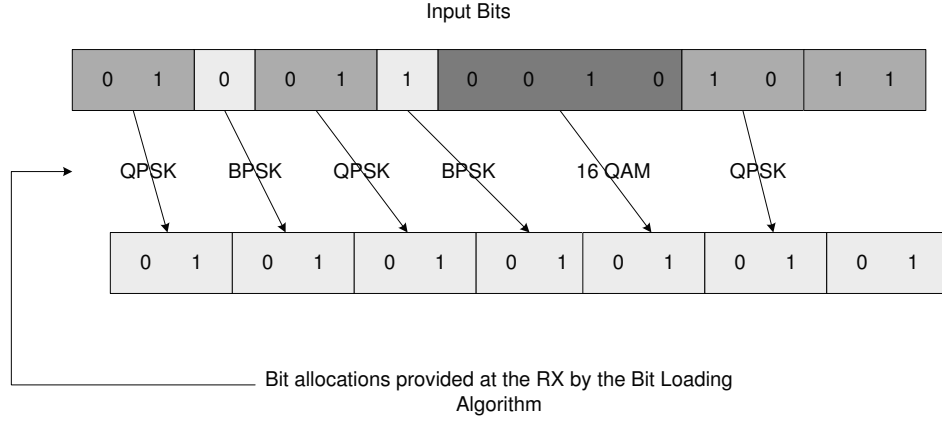


Figure 2.6. Example Showing Bit Allocations by a Bit Loading Algorithm

precise knowledge of the flat fading channel gain for each subcarrier. A substantial performance improvement can be obtained in this adaptive modulation application, where the modulator basis functions are designed as a function of measured channel characteristics. On a good subchannel (high SNR), modulation methods such as 64 QAM are used to increase the bit rate per symbol and a lower modulation such as QPSK is performed on a poor subchannel to keep the error rate low.

2.1.1.4 OFDM Reception

Two important components for processing of the received OFDM signal are synchronization and channel estimation.

Synchronization

At the front-end of the receiver OFDM, signals are subject to synchronization errors due to oscillator impairments and sample clock differences [15]. The demodulation of the received radio signal to baseband, possibly via an intermediate frequency (IF), involves oscillators whose frequencies may not be perfectly

aligned with the transmitter frequencies. This results in a carrier frequency offset. Also, demodulation (in particular, the radio frequency demodulation) usually introduces phase noise acting as an unwanted phase modulation of the carrier wave. Carrier frequency offset and phase noise degrade the performance of an OFDM system.

When the baseband signal is sampled at the Analog-to-Digital converter, the sample clock frequency at the receiver may not be the same as that at the transmitter. Not only may this sample clock offset cause errors, it may also cause the duration of an OFDM symbol at the receiver to be different from that at the transmitter. Since the receiver needs to determine when the OFDM symbol begins for proper demodulation with the FFT, a symbol synchronization algorithm at the receiver is usually necessary. Symbol synchronization also compensates for delay changes in the channel.

The most important effect of a frequency offset between transmitter and receiver is a loss of orthogonality between the subcarriers resulting in ICI. The characteristics of this ICI are similar to white Gaussian noise and lead to a degradation of the SNR. For both additive white Gaussian noise channels (AWGN) and fading channels, this degradation increases with the square of the number of subcarriers.

Finally, the degradation due to symbol timing errors is not graceful. If the length of the cyclic prefix exceeds the length of the channel impulse response, a receiver can capture an OFDM symbol anywhere in a region where the symbol appears cyclic, without sacrificing orthogonality. A small error only appears as pure phase-rotations of the data symbols and may be compensated for by the channel equalizer, still preserving the system's orthogonality. A large error resulting in

capturing a symbol outside this allowable interval, on the other hand, causes ISI, ICI, and a performance degradation.

Time and frequency offset estimators have been addressed in a number of publications [19]. We divide these estimators conceptually into two groups. The first group assumes that transmitted data symbols are known at the receiver. This can, in practice, be accomplished by transmitting known pilot symbols according to some protocol. The unknown symbol timing and carrier frequency offset may then be estimated from the received signal. The insertion of pilot symbols usually implies a reduction of the data rate.

A second approach uses statistical redundancy in the received signal. The transmitted signal is modeled as a Gaussian process. The offset values are then estimated by exploiting the intrinsic redundancy provided by the L samples constituting the cyclic prefix. The basic idea behind these methods is that the cyclic prefix of the transmitted signal yields information about where an OFDM symbol is likely to start. Moreover, the transmitted signal's redundancy also contains useful information about the carrier frequency offset.

Channel Estimation

In an OFDM link, the data bits are modulated on the subcarriers by some form of PSK or QAM. To estimate the bits at the receiver, knowledge is required about the reference phase and amplitude of the constellation on each subcarrier. In general, the constellation of each subcarrier shows a random phase shift and amplitude change, caused by carrier frequency offset, timing offset, and frequency selective fading. To cope with such variations, two methods exist. One is coherent detection, which uses estimates of the reference amplitudes and phases to determine the best possible decision boundaries for the constellation of each

subcarrier. Of all the modulation techniques which lend themselves to coherent detection, those that are most commonly found in present-day applications are the quadrature modulations which include QPSK, quadrature amplitude shift keying (QASK), and quadrature partial response (QPR) [20]. The second approach is differential detection, which does not use absolute reference values, but only looks at the phase and/or amplitude differences between two QAM values. Differential detection can be done both in the time domain and in the frequency domain. These systems use differential modulation schemes such as differential phase-shift keying (DPSK), where, this scheme encodes the transmitted information into phase differences from symbol to symbol.

In a fading channel environment, differential modulation does not need to track the subcarrier attenuations. The performance sacrifice associated with this modulation scheme compared with coherent modulation schemes is often motivated by its simple receiver structure and its avoidance of pilot symbols. However, if the subcarriers are coherently modulated as in the digital video broadcasting project(DVB) standard, estimation of the channel's attenuations of each subcarrier is necessary. These estimates are used in the channel equalizer, which in an OFDM receiver, may consist of one complex multiplication for each subcarrier in an OFDM symbol.

To be able to interpolate the channel estimates both in time and frequency from the available pilots, the pilot spacing has to fulfill the nyquist sampling theorem, which states that the sampling interval must be smaller than the inverse of the double-sided bandwidth of the sampled signal. By choosing the pilot spacing much smaller than these minimum requirements, a good channel estimation can be made with a relatively easy algorithm. The more pilots used, however, the

smaller the effective SNR becomes that is available for data symbols. Hence, the pilot density is a tradeoff between channel estimation performance and SNR loss.

To determine the minimum pilot spacing in time and frequency, we need to find the bandwidth of the channel variation in time and frequency. These bandwidths are equal to the Doppler spread B_d in the time domain and the maximum delay spread τ_{max} in the frequency domain [21]. Hence, the requirements for the pilot spacing's in time and frequency s_t and s_f are:

$$s_t \leq 1/B_d \quad (2.3)$$

$$s_f \leq 1/\tau_{max}. \quad (2.4)$$

Channel estimation in OFDM is usually performed with the aid of pilot symbols. Since each subcarrier is flat fading, techniques from single-carrier flat fading systems can be applied to OFDM. For such systems, pilot-symbol assisted modulation (PSAM) on flat fading channels involves the sparse insertion of known pilot symbols in a stream of data symbols. The attenuation of the pilot symbols is measured and the attenuations of data symbols between these pilot symbols are typically estimated and interpolated using time-correlation properties of the fading channel [22].

In OFDM systems where Doppler effects are kept small (i.e., the OFDM symbol is short compared with the coherence time of the channel), the time correlation between the channel attenuation of consecutive OFDM symbols is high. Furthermore, in a properly designed OFDM system, the subcarrier spacing is small compared with the coherence bandwidth of the channel. Therefore, there also exists some substantial frequency correlation between the channel attenuation of adjacent subcarriers. Both the time and frequency correlations can be exploited by a

channel estimator. The choice of pilot pattern determines the form of the channel estimator.

Channel estimation techniques consist of two steps: First, the attenuation at the pilot positions is measured and possibly smoothed using the channel correlation. These measurements then serve to estimate (interpolate) the complex-valued attenuation of the data symbols in the second step. The second step uses the channel correlation properties, either with interpolation filters or with a decision-directed scheme. Depending on the pilot pattern the estimation strategies diverge in this second step.

Once we have the channel information estimated, we can remove the negative effects of the channel from the receive signal by using one of three general equalization techniques: the maximum likelihood sequence estimation (MLSE), linear equalizers, and decision feedback equalizers. We only need one tap equalizer for each subcarrier. This makes the linear equalizer method the logical choice. We can determine the coefficient of the equalizer by using either the minimum mean square error (MMSE) or the zero forcing (ZF) criteria. The latter works as follows:

$$\hat{H}_n = \frac{Y_n}{P_n} = H_n + \frac{N_0}{P_n}, \quad (2.5)$$

where, Y_n is the receive signal, P_n represents the pilot symbols and N_0 is the additive white Gaussian noise.

Channel estimation inverts the effect of nonselective fading on each subcarrier. Usually OFDM systems provide pilot signals for channel estimation. In the case of time-varying channels, the pilot signal should be repeated frequently. The spacing between pilot signals in time and frequency depends on coherence time and bandwidth. Throughout this thesis, the channel estimates are assumed to be

perfect, and available to both the transmitter and receiver. Given full knowledge of the channel, the transmitter and receiver can determine the frequency response of the channel, and the channel gains at each tone of the OFDM symbol. Given these gains, the adaptive algorithm can proceed to calculate the optimal bit and power allocation.

2.2 MIMO-OFDM

Multiple input multiple output (MIMO) systems use multiple transmit and receive antennas to improve the capacity of the system [5]. The multiple antennas can be used to increase data rates through multiplexing, or to improve performance through diversity. This technique can significantly increase the data rates of wireless systems without increasing transmit power or bandwidth. The cost of the performance enhancements obtained through MIMO techniques is the added cost of deploying multiple antennas, the space and power requirements of these extra antennas (especially on small handheld units), and the added complexity required for multidimensional signal processing [23].

A great deal of research work has been devoted to the area of combining this spatial scheme with OFDM systems. This system combines the advantages of both techniques in providing simultaneously increased data rate and elimination of the effects of delay spread. Power control for subcarriers on a MIMO/OFDM system can be crucial in enhancing the spectral and power efficiency. Without any interference, the best power control to optimize the transmission is the waterfilling solution. But since it is not practically feasible, we have employed the adaptive loading algorithm described in the next section [24]. This section concentrates on the concept employed in this thesis, that every matrix channel can be

decomposed into a set of parallel subchannels over which data can be transmitted independently, given appropriate precoding and shaping transformations at the transmitter and receiver, respectively [25].

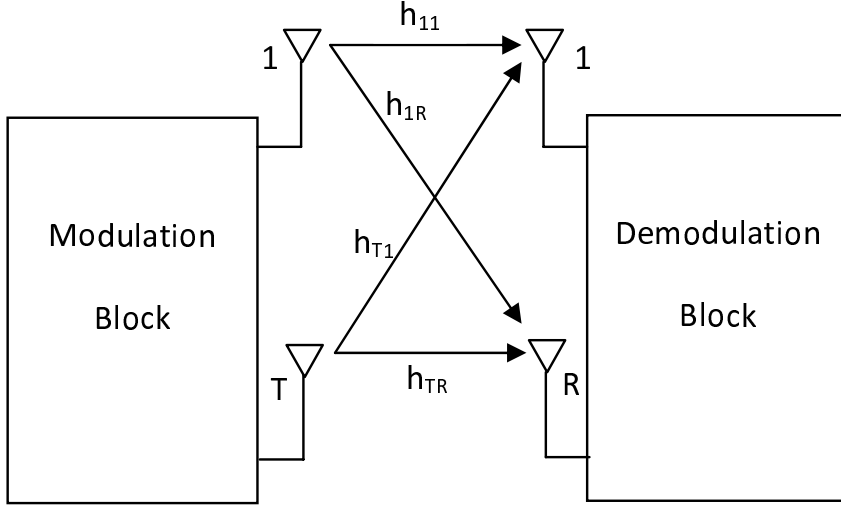


Figure 2.7. MIMO System With T Transmit Antennas and R Receive Antennas.

Shown in Figure 2.7 is a MIMO transmit/receive system with T transmit antennas and R receive antennas. This system can be represented simply as $y = Hx + n$. Here x represents the T -dimensional transmitted symbol, n is the R -dimensional noise vector, and H is the $R \times T$ matrix of channel gains h_{ij} representing the gain from transmit antenna j to receive antenna i .

If we consider the case of perfect channel state information at the transmitter and receiver, we can decompose the MIMO channel on each tone into R parallel non-interfering single input single output (SISO) channels using the singular value decomposition (SVD) [18]. This results in the performance gain called multiplexing gain. By multiplexing data onto these independent channels, we get an R -fold increase in data rate in comparison to a system with just one antenna at

the transmitter and receiver. This increased data rate is called the multiplexing gain.

Consider the MIMO system shown above in Figure 2.7. For any matrix H we can obtain its SVD as:

$$H = U\Sigma V^H \quad (2.6)$$

where the $R \times R$ matrix U and $T \times T$ matrix V are unitary matrices and Σ is $R \times T$ diagonal matrix of singular values of H .

Now, if we use a transmit precoding filter of V and a receiver shaping filter of U , the equivalent MIMO channel between the IFFT and FFT blocks decomposes into parallel subchannels. Note that the number of such subchannels is exactly equal to the number of nonzero singular values of H . This same decomposition applies to each subchannel of the OFDM system. In general each precoder and shaping matrix will be different for different subchannels [26].

Given the decomposition outlined above, the adaptively modulated MIMO/OFDM system requires that each subchannel has the corresponding precoder and shaping matrix applied to it. In other words, the MIMO/OFDM adaptive modulation problem decomposes into a bit loading over all the nonzero singular values of all the tones. Thus, the problem will be larger than in the SISO case, but the decomposition has allowed us to proceed without any changes in the optimization algorithm to be employed.

2.3 Channel Model

Designing future mobile radio systems requires a comprehensive knowledge about propagation characteristics over different types of environments. Propagation studies involving the creation of channel models and their statistical parameters could be used to design better wireless systems.

Indoor radio channel environments are prone to interference due to reflection, refraction and scattering of radio waves by structures inside a building. Transmitted signals often reach the receiver via multiple paths resulting in a phenomenon known as *multipath fading*. Multipath fading causes improper detection of the signal across the frequency domain which can seriously degrade the system performance. If we can adequately characterize the channel, appropriate transmitter settings combined with equalizers can be employed. Therefore, developing a propagation model to predict the characteristics of a wireless channel environments is important.

Radio propagation channel models can be classified into two major classes: *statistical models* and *site specific propagation models* [27]. Statistical models rely on measurement data and follow statistical impulse response modeling of the multipath fading channel. The goal of statistical modeling is to investigate the distribution of various channel characteristics such as *arrival time*, *amplitude and phase sequences*, *inter-relation between path variables*, and *spatial correlations on path variables*. In contrast, site specific propagation models are based on the use of electromagnetic wave propagation theory to characterize indoor radio propagation. This technique has been proposed to predict *path loss*, *time invariant impulse response* and *rms delay spread*.

Saleh and Valenzuela used their measurement results from a medium-sized two

story office buildings together, with results from other researchers, developed a model for indoor radio channel simulation and analysis of various communication schemes [28]. The model was shown to fit the measurements and may be extended to other buildings by adjusting its parameters. They effectively measured the impulse response of the channel by transmitting and receiving a sequence of narrow pulses from omnidirectional antennas. Based on these time-domain measurements, they presented a model that describes the wireless channel as the sum of discrete arrivals, each with a different delay in its arrival time.

The complicated random and time varying indoor radio propagation channel can be modeled by assigning linear time variant an impulse response to each point in the 3-D space given by [27]:

$$h(t, \tau) = \sum_{k=0}^{N(\tau)-1} \beta_k(t) \delta[\tau - \tau_k(t)] e^{j\theta_k(t)} \quad (2.7)$$

where t and τ are the observation time and application time of an impulse, $N(\tau)$ is the number of multipath components, and $\beta_k(t)$, $\tau_k(t)$, and $\theta_k(t)$ are the random time-varying amplitude gain, arrival time and phase sequence and $\delta[\cdot]$ is the Dirac delta function. A time-invariant version of this model which is successfully used in many radio applications given by [28]:

$$h(t) = \sum_k \beta_k e^{j\theta_k} \delta(t - \tau_k) \quad (2.8)$$

Due to the motion of people and equipment in and around the building, the parameters β_k , τ_k , and θ_k are randomly time-varying functions. However, the rate of their variations is very slow compared to any useful signaling rates that are likely to be considered, e.g., higher than tens of kbit/s. Thus, these parameters can be treated as virtually time-invariant random variables.

The model starts with the assumption that the multipath components arrive

in clusters. The formation of the clusters is related to building structure, while the multipath components within each cluster are formed by multiple reflections from objects in the vicinity of transmitter and receiver. The cluster arrival times, i.e., the arrival times of the first rays of the clusters, are modeled as a Poisson arrival process with some fixed rate Λ . Within each cluster, subsequent rays also arrive according to a Poisson process with another fixed rate λ . Typically, each cluster consists of many rays, i.e., $\lambda \gg \Lambda$.

Let the gain of the k th ray of the l th cluster be denoted by β_{kl} and its phase by θ_{kl} . Thus, instead of Eq. (2.8), complex low pass impulse response of the channel is given by [28]:

$$h(t) = \sum_{l=0}^{\infty} \sum_{k=0}^{\infty} \beta_{kl} e^{j\theta_{kl}} \delta(t - T_l - \tau_{kl}), \quad (2.9)$$

where T_l is the arrival time of l th cluster and τ_{kl} is the arrival time of k th ray measured from the beginning of l th cluster. Both of these variables are described by the independent inter arrival exponential probability density functions as [28]:

$$p(T_l|T_{l-1}) = \Lambda \exp[-\Lambda(T_l - T_{l-1})], \quad l > 0, \quad (2.10)$$

$$p(\tau_{kl}|\tau_{(k-1)l}) = \lambda \exp[-\lambda\tau_{kl} - \tau_{(k-1)l}], \quad k > 0. \quad (2.11)$$

The received amplitude gains, β_{kl} of each component are independent Rayleigh random variables with a variance that decays exponentially with the propagation delay, and as well as with time delay, within a cluster. Thus, these amplitude gains can be computed as [28]:

$$\begin{aligned}
\overline{\beta_{kl}^2} &\equiv \overline{\beta_{T_l, \tau_{kl}}^2} \\
&= \overline{\beta_{0,0}^2} e^{-T_l/\Gamma} e^{-\tau_{kl}/\gamma},
\end{aligned} \tag{2.12}$$

where $\overline{\beta_{0,0}^2} = \overline{\beta_{00}^2}$ is the average power gain of the first ray of the first cluster, and Γ and γ are power-delay time constants for the clusters and the rays, respectively.

The actual arrival amplitudes are then described as a Rayleigh random variable with a time-varying mean given by the double exponential. The phase of each arrival is determined by the length of the path traveled, the medium through which the signal passes, and by the reflection coefficients of the scattering surfaces. The corresponding phase angles, θ_{kl} for each component are independent uniform random variables over $[0, 2\pi]$, the reason is that phases are very sensitive to even a small variation e.g., movement of the order of millimeter. The model has enough flexibility to permit reasonably accurate fitting of the measured channel response is simple enough for simulation.

Figure 2.8 is a schematic representation of the channel model from [28]. Figure 2.8 (a) illustrates the exponentially decaying ray and cluster average powers as described in Eq. (2.12). Figure 2.8 (b) shows the realization of a channel impulse response generated taking into consideration, all the parameters described.

This multipath channel model is flexible enough to fit the experimental data reasonably well, while retaining the basic features of a constant-rate Poisson arrival-time process and mutually independent path gains, thus making its use in analysis relatively simple. In addition, the model can be explained from a physical viewpoint, thus making it more readily extendable to other types of environments.

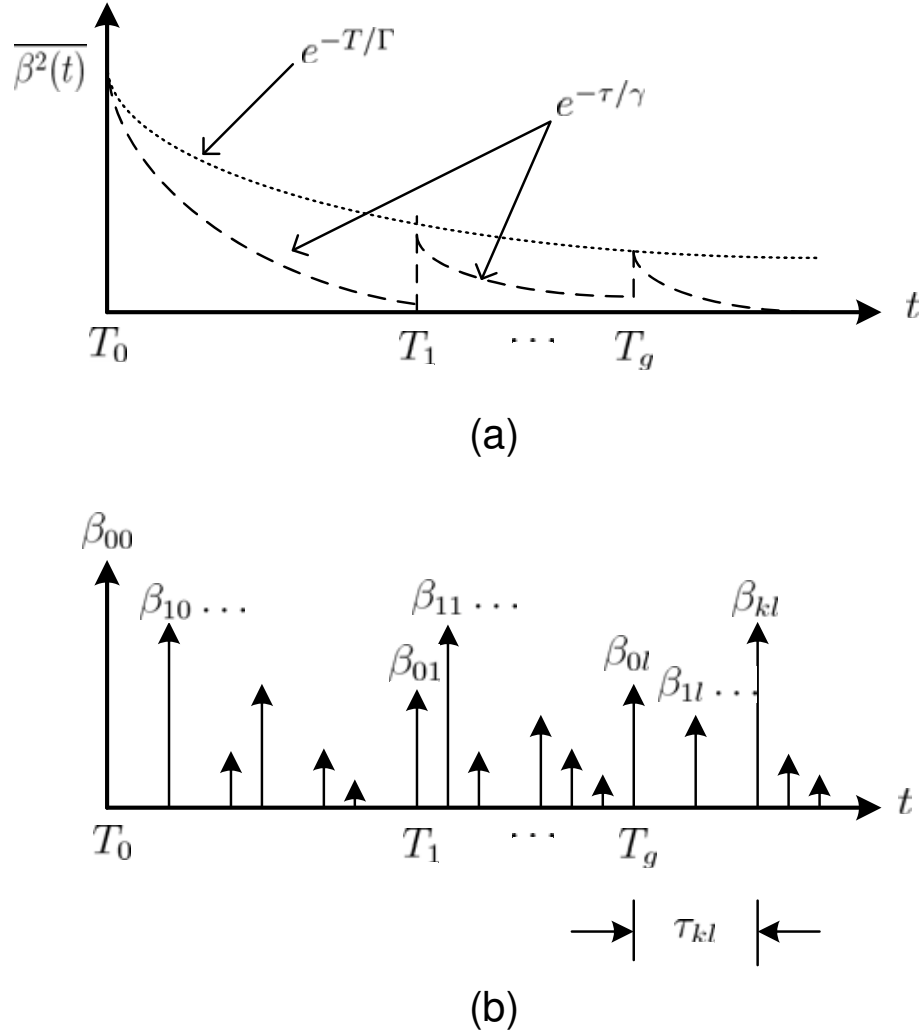


Figure 2.8. A Schematic Illustration of Channel Model. (a) Exponentially Decaying Ray and Cluster Average Powers. (b) Channel Impulse Response (from [28]).

2.3.1 Time-Varying Channel Correlation Models

In wireless transceiver systems, time varying channels are often encountered. Depending on the surroundings, atmosphere, etc., successive instances of the channel impulse response can possess some degree of correlation. In probability theory and statistics, *correlation* indicates the strength and direction of a linear relation-

ship between two random variables. The time correlation between two random variables can be introduced using the equation shown below, which is the channel model generation *via* the time domain recursion:

$$h'(t) = \alpha h(t) + (1 - \alpha)h(t - 1) \quad (2.13)$$

where $h(t)$ represents current channel impulse response at time t , $h(t - 1)$ represents previous channel impulse response at time $t - 1$, α represents the correlation percentage being introduced between the current and previous channel estimate, and $h'(t)$ represents the correlated channel response.

The time-varying channels can range from very slowly varying channels with 99% correlation to faster varying uncorrelated channel. The practicality of adaptive signaling in real world implementation has been questioned due to the variation of the wireless channel over time, which results in a different channel at the time of data transmission than at the time of channel estimation. Thus, this thesis investigates the performance of these systems for a range of correlation values [29, 30].

A completely uncorrelated time varying channel is shown in Figure 2.9. We can see that each time instance of the channel is different from the next instance. There is no repetition or redundancy when two channel time instances are compared. Figure 2.10 shows strong time correlation, i.e., 99% correlation between the channel instances.

We can see in Figure 2.10 how each channel time instance consists of 99% of the previous channel instance and only 1% of the new channel instance. Since the time variation is very low in these channels, they are called slow time varying channels. Figure 2.11 shows the response with channel instances having 95%

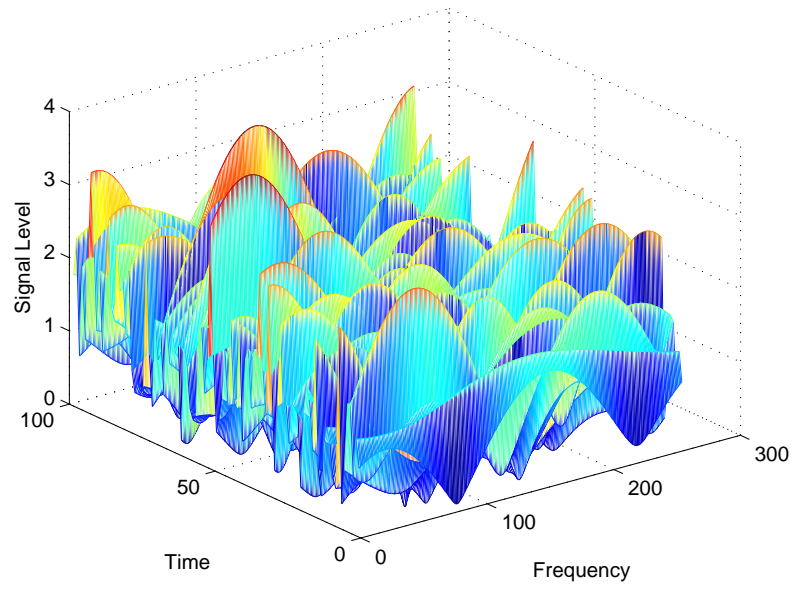


Figure 2.9. Uncorrelated Time-varying Channel Model

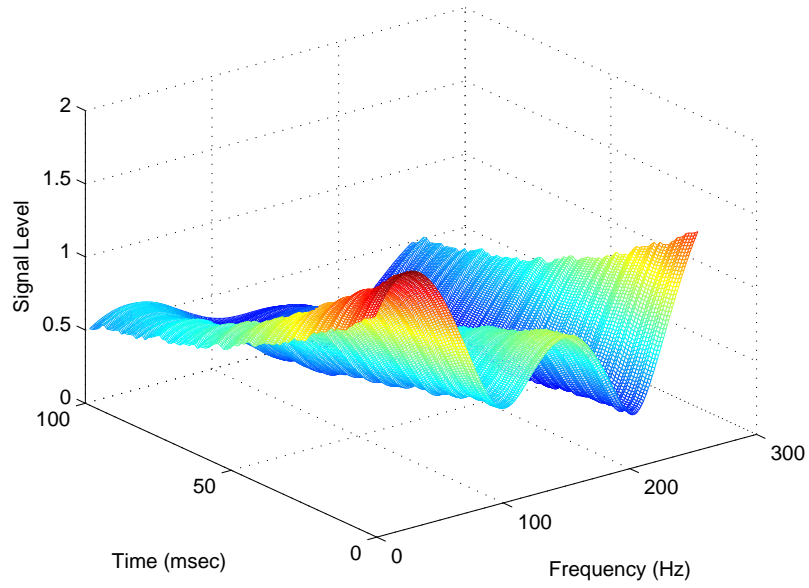


Figure 2.10. 99% Correlated Time-varying Channel Model

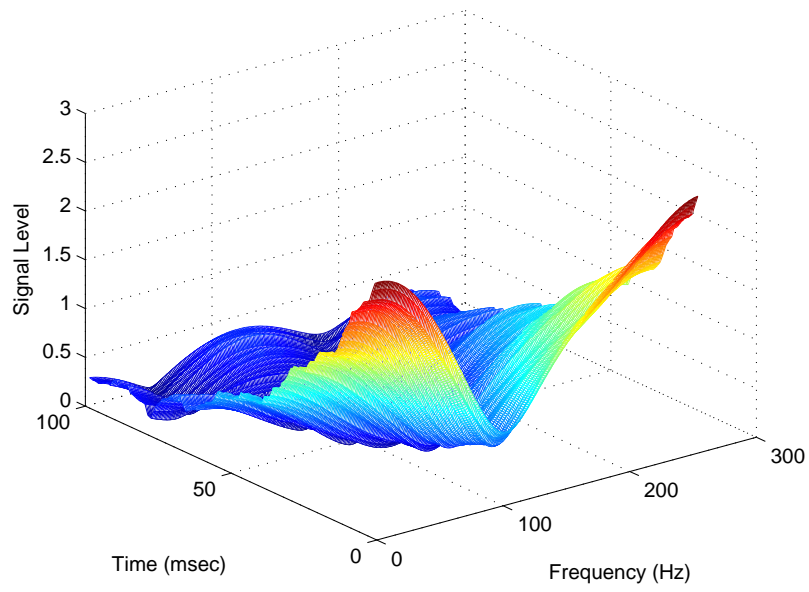


Figure 2.11. 95% Correlated Time-varying Channel Model

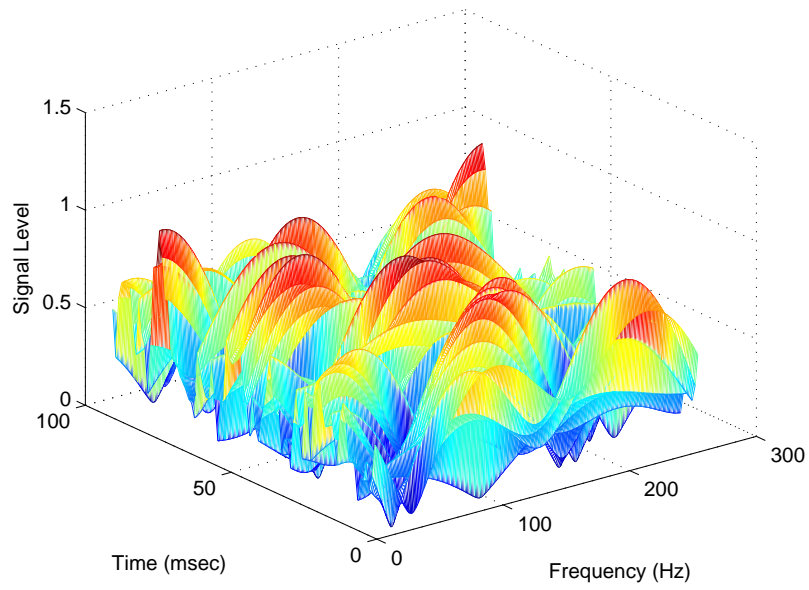


Figure 2.12. 85% Correlated Time-varying Channel Model

correlation with each other and Figure 2.12 shows the channel instances with 85% correlation with each other.

2.4 Quantization

Since quantization has been used in feedback data compression, a brief summary of quantization methods is given in this section.

Message signals such as speech waveforms or video waveforms have a continuous amplitude range. When such continuous amplitude samples are transmitted over a noisy channel, the receiver cannot discern the exact sequence of transmitted values. The effect of the noise in the system can be minimized by representing the samples by a finite number of predetermined levels and transmitting the levels using a signalling scheme such as PAM, QAM etc.

Quantization refers to the process of representing the analog sampled values by a finite set of levels. While sampling converts a continuous time signal to a discrete time signal, quantizing converts a continuous amplitude sample to a discrete amplitude sample. Thus, sampling and quantizing convert the output of an analog information source into a sequence of levels or symbols [31].

There are two types of quantization — scalar quantization and vector quantization. In scalar quantization, each input symbol is treated separately in producing the output, while in vector quantization the input symbols are grouped together into vectors and processed to give the output. This grouping of data and treating them as a single unit increases the optimality of the vector quantizer compared to scalar quantizer, but at the cost of increased computational complexity. Here, we'll take a look at scalar quantization [32].

A quantizer can be specified by its input partitions and output levels, called

reproduction points. If the input range is divided into levels of equal spacing, then the quantizer is called a uniform quantizer. Otherwise, it is called a nonuniform quantizer. A uniform quantizer can be easily specified by its lower bound and the step size. The measure of performance that is most commonly used for evaluating the performance of a quantizing scheme is the output signal to quantizing noise power ratio.

The optimum quantizer encoder and optimum decoder must satisfy the following conditions [33]:

- Given the output levels or partitions of the encoder, the best decoder is one that puts the reproduction point's x' on the centers of mass of the partitions. This is known as *centroid condition*.
- Given the reproduction points of the decoder, the best encoder is one that puts the partition boundaries exactly in the middle of the reproduction points, i.e., each x is translated to its nearest reproduction point. This is known as *nearest neighbor condition*.

The quantization error $(x - x')$ is used as a measure of optimality of the quantizer encoder and decoder.

Uniform Quantization

In uniform quantization, all quantization regions are of equal step size (Δ), except the first and last regions, if samples are not finite valued. With N quantization regions, $\log_2(N)$ bits are used to represent each quantized value. The uniform quantizer yields the highest (optimum) average signal to quantizer noise power ratio at the output if the signal has a uniform probability density function (pdf), and doesn't work well when the signal has nonuniform pdf. Also, a fixed

step size will produce relatively larger quantization error when the signal is small, and hence, will adversely affect signal quality when the input signal has smaller amplitude.

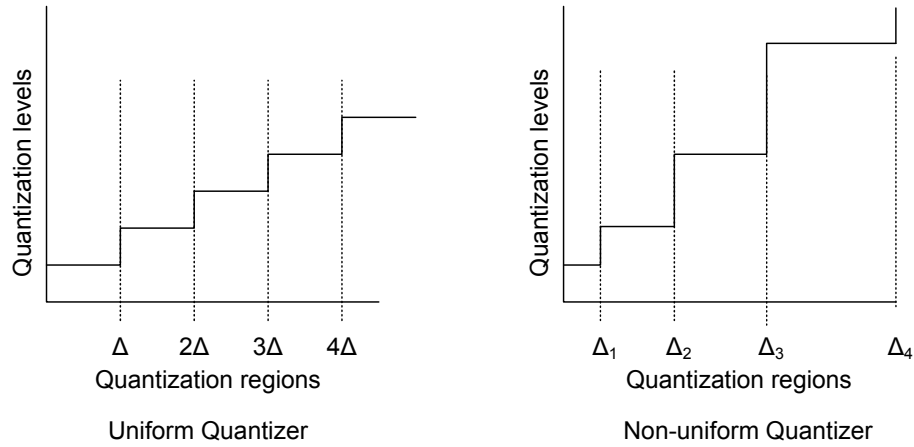


Figure 2.13. Uniform and Nonuniform Quantizers

Nonuniform Quantization

A better scheme for quantizing a random variable with a nonuniform pdf is to use quantizing scheme that use a variable step size, Δ_i , which has smaller values when signal amplitude is small and larger values when the signal amplitude is large. If a uniform quantizer is used in this case, it yields the same peak error in each quantizer bin, which means smaller signals will suffer a larger relative errors compared to larger signal values. But a nonuniform quantizer will yield a higher average signal to quantizing noise power ratio than the uniform quantizer. Here, quantization values should be the “centroid” of their regions, i.e., the conditional expected value of that region. For a given number of levels, the nonuniform quantizer yields a smaller MSE. Shown in Figure 2.13 is the illustration of the length of quantization regions in uniform and nonuniform quantizers. As we can see the uniform quantizer chose equal quantization levels and the nonuniform

quantizer chose unequal quantization regions basing on signal pdf. Nonuniform quantizers are difficult to implement because this requires knowledge of source statistics and different quantizers for different input types.

One proposed solution for such problems was converting the nonuniform pdf signal to a uniform pdf signal using compander and then applying uniform quantizer. The idea behind this compander is, that initially, compression transforms the input variable X (with nonuniform pdf) to another variable Y using a non-linear transformation $Y = g(X)$, such that $f_Y(y)$ has a uniform pdf. Then Y is uniformly quantized and transmitted. At the receiver, a complementary expander with transfer characteristics g^{-1} restores the quantized values of X . The compressor and expander together are called compander.

The results achieved are optimal when the quantization applied to the data is uniform and its followed by lossless compression algorithms. Thus, this thesis would be concentrating on uniform quantization and lossless data compression techniques.

2.5 Data Compression Techniques

The basic definition of data compression is “reducing the amount of data required to represent a source of information while preserving the original content as much as possible” [34]. There are two kinds of data compression algorithms, lossy data compression and lossless data compression.

In *lossy data compression*, the original message can never be recovered exactly as it was before it was compressed. As the name indicates, there will be some loss of the original information. It is not good for critical data, when we cannot afford to lose even a single bit. It is used mostly in sound, video, image compressions

where the losses can be tolerated. Some lossy data compression schemes are Vector Quantization, JPG, MPEG etc.

In *lossless compression*, the original message can be exactly decoded. This lossless compression is achieved by finding repeated patterns in a message and encoding them in an efficient manner; this is also referred to as ‘redundancy reduction. Popular algorithms of this kind are: Lempel-Ziv-Welch (LZW) [35,36], Run Length Encoding (RLE), Huffman coding [37], and Arithmetic Coding [38].

Choosing an adequate compression algorithm is very important in this thesis, since our main aim is to compress the feedback information using one of the above lossless algorithms and at same time never lose any of it (since if we cannot recover the original data after compression, that would lead to bad system performance).

Thus, in this thesis we will have to choose lossless compression algorithms. Specifically the RLE, Huffman Coding, and LZW compression schemes have been employed in this work.

2.5.1 Huffman Coding

Huffman compression, also known as Huffman encoding, is one of many and one of the most famous compression techniques in use today [37]. One of the main benefits of Huffman compression is its ability to be implemented easily and to achieve a decent compression ratio.

The Huffman compression algorithm assumes data files consist of some symbol values that occur more frequently than other symbol values in the same file. The most common characters in the input file (i.e., characters with higher probability) are assigned short binary codes. Least common characters (i.e., those with lower probabilities) are assigned longer binary codes. By analyzing the data, the

algorithm builds a dictionary initially using the probability of occurrence of each symbol, which associates each data symbol with a codeword, which has the property that no codeword in the dictionary is a prefix of any other codeword in the dictionary.

For example, consider a data source that produces “1” values with probability 0.1, “2” values with probability 0.1, and “3” values with probability 0.8. By having this statistical information about the source, Huffman encoding and decoding can be done easily.

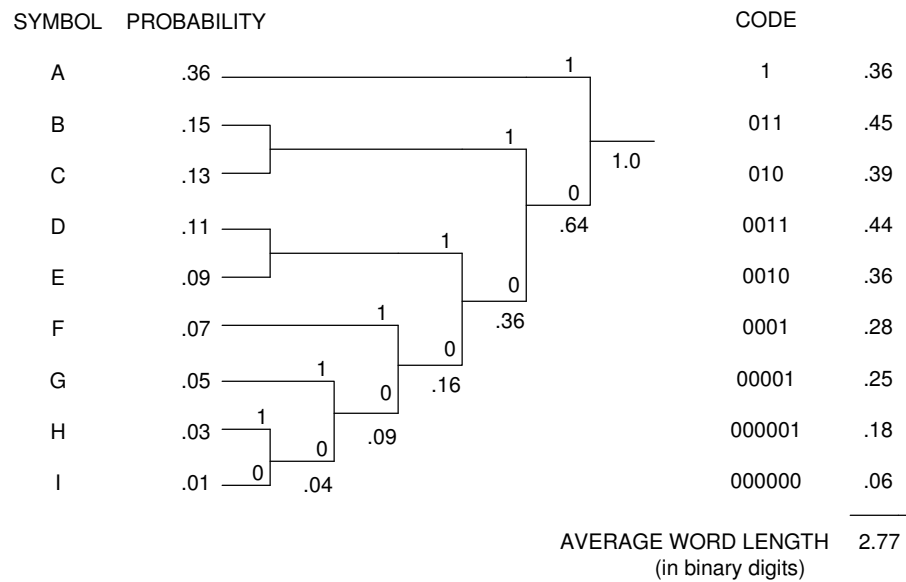


Figure 2.14. Huffman Coding Example

A Huffman coding example is shown in Figure 2.14. We can see that the symbols are arranged in the descending order of their occurrence based on probability. Then a binary tree is generated from left to right starting with the two least probable symbols. The least probable symbols are combined to form another equivalent symbol having a probability that equals the sum of the two symbols. This is done until we are left with one single symbol. Then, by reading the tree

from right to left, different codes are assigned to each symbol as shown in the above example.

The first problem with Huffman coding is that the size of input symbols is limited by the size of the translation table needed for the compression. That is, a table is needed that lists each input symbol and its corresponding code. If a symbol is one eight-bit byte, then a table of 256 entries is sufficient. Such a table saves on storage costs but limits the degree of compression achieved.

The second problem with Huffman encoding is the complexity of the decompression process. The length of each code to be interpreted for decompression is not known until the first few bits are interpreted. The basic method for interpreting each code is to interpret each bit in a sequence and choose a translation subtable according to whether the bit is a one or a zero.

A third issue with Huffman encoding is that we need to know the frequency distribution for the ensemble of possible input symbols. A common solution is to analyze each data block individually to adapt the character distribution uniquely to that block. We must make two passes over the data, (1) a pass to count characters and perform a sort operation on the character table, and (2) a pass for encoding. This adaptable approach is acceptable if high transfer rates through the compressor are not required and if the data blocks being compressed are very large relative to the size of the translation table.

2.5.2 Run Length Encoding (RLE)

Run length encoding (RLE) stands out from other methods of compression, since it does not try to reduce the average symbol size compared to Huffman coding or Arithmetic coding, and it doesn't replace strings with dictionary references such

as Lempel-Ziv and Lempel-Ziv-Welch style coding [35,36]. RLE replaces a string of repeated symbols with a single symbol and a count (i.e., run length) indicating the number of times the symbol is repeated. It is called run length because a “run” is made for repeated bits and coded in lesser bits by only stating how many bits were there.

The problem with run length encoding for character sequences intermixed with other data is in distinguishing the count fields from normal characters, which may have the same bit patterns. This problem has several solutions, but each one has disadvantages. For example, a special character might be used to mark each run of characters, which is fine for ASCII text, but not for arbitrary bit patterns such as those in binary integers. Typically, three characters are needed to mark each character run, so this encoding would not be used for runs of three or fewer characters.

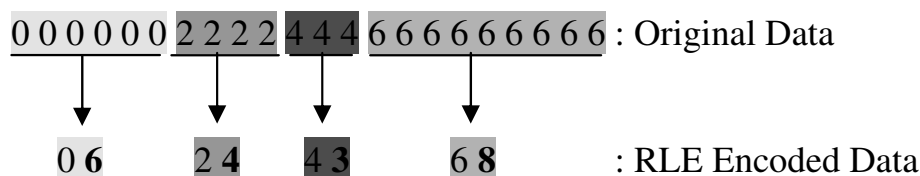


Figure 2.15. RLE Coding Example

Shown in Figure 2.15 is an example of RLE encoding. In the original data we can see a series of repetitions on particular symbol, and when such repetition occurs, RLE encoding replaces the whole repeating string of symbols with an actual symbol and its count of repetition. The numbers represented in bold are the repetition count values i.e., the number of times the particular symbol has repeated. The next step in this compression technique would be to convert each of the decimal values of run into 4-bit binary values, or nibbles. The only unique rule

to follow during this conversion comes into play when one encounters a decimal value of 15 or greater. Since the largest decimal number that a 4-bit binary nibble can represent is 15 (which corresponds to four binary 1's — 1111), one must convert a run/decimal value that is greater than 15 into multiple 4-bit nibbles. For example, a run of 20 would be converted into 1111 1010, in which the first nibble is the value 15, and the second nibble is the value 5. A caveat to this rule is that if you are converting the value 15 itself, then you would also create two nibbles: 1111 followed by 0000. The reason for this is simply to be consistent, so that whenever a binary nibble of 1111 is encountered, the following nibble is added to the value of 15. So, the higher the decimal values, the larger is number of binary nibbles required for representation. One disadvantage of this technique is that it is worthwhile only if the original data consist predominantly of binary 0's.

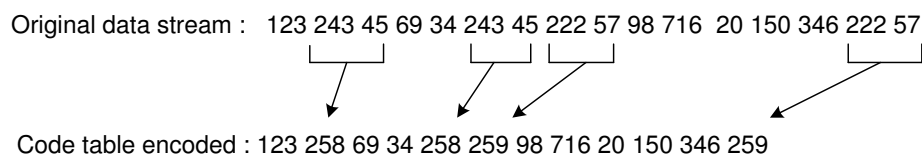
2.5.3 LZW Compression

There are several compression algorithms that use a “dictionary,” or code book, known to both the coder and the decoder, which is generated during the coding and decoding processes. Many of these build on work reported in 1978 by Abraham Lempel and Jacob Ziv, and are known as “Lempel-Ziv” (LZ) encoders [35]. These coders replace repeated occurrences of a string by references to an earlier occurrence. The dictionary is merely the collection of these earlier occurrences.

One widely used LZ algorithm is the Lempel-Ziv Welch (LZW) algorithm described by Terry A. Welch [36]. This algorithm was originally designed to minimize the number of bits sent to and from disks, but it has been used in many contexts, including GIF compression programs for images. The LZW compression

algorithm is “reversible,” meaning that it does not lose any information – the decoder is able to reconstruct the original message exactly.

The Lempel-Ziv algorithm converts variable-length strings of input symbols into fixed length of predictable codes. The symbol strings are selected so that all have nearly equal probability of occurrence. Consequently, strings of frequently occurring symbols will contain more symbols than a string having infrequent symbols. This form of compression is effective at exploiting character frequency redundancy, character repetitions and high-usage pattern redundancy. However, it is not effective on positional redundancy, i.e., a symbol repeating itself occasionally [36].



	Code no.	Transalation
	0000	0
	0001	1
	.	.
	.	.
	0255	255
U N I Q U E	0258	243 45
	0259	222 57
	.	.
	.	.
	4096	xxx xxx

Figure 2.16. Illustration of LZW Compression

This type of algorithm is adaptive in the sense that it starts with an empty table of symbol strings and builds the table during both the compression and decompression process. These are one-pass procedures that require no prior information about the input data statistics, and the execution time is proportional

to the length of the message. This adaptivity results in poor compression during the initial portion of each message. As a result, the message must be long enough for the procedure to build sufficient symbol frequency experience to achieve good compression over the full message. On the other hand, most finite implementations of an adaptive algorithm lose the ability to adapt after a certain amount of the message is processed. If the message is not homogenous and its redundancy characteristics shift during the message, then compression efficiency declines if the message length significantly exceeds the adaptive range of the compression implementation.

An example of LZW compression is shown in Figure 2.16, where the codes are assigned starting from 258, as 256 is reserved for indicating start of transmission and 257 for end of transmission. We can see a string of symbols occurring frequently. Such strings were replaced by the LZW codes, and the final codes and their translations are also shown in the above figure. The LZW method achieves compression by using codes 256 through 4095 to represent sequences of bytes. For example, code 523 may represent the sequence of three bytes: 231 124 234. Each time the compression algorithm encounters this sequence in the input file, code 523 is placed into the encoded file. During decompression, code 523 is translated via the code table to recreate the true 3 byte sequence. The longer the sequence assigned to a single code, and the more often the sequence is repeated, the higher the compression achieved.

LZW is distinguished by its very simple logic, which yields relatively inexpensive implementations. The real difficulty lies in the efficient management of the code table. The brute force approach results in large memory requirements and a slow program execution. Several tricks are used in commercial LZW programs

to improve their performance. For instance, the memory problem arises because it is not known beforehand how long each of the character strings for each code will be. Most LZW programs handle this by taking advantage of the redundant nature of the code table. The execution time of the compression algorithm is limited by searching the code table to determine if a match is present. There are many schemes for this type of code table management, and they can become quite complicated. These quantization and compression schemes are applied to the feedback data, i.e., generated by adaptive bit loading algorithms.

2.6 Chapter Summary

In this chapter the concepts of OFDM and MIMO-OFDM have been explained in detail. We learned the basic concepts that make OFDM work and how to overcome interference such as ISI and ICI with the use of a cyclic prefix. Also, a solution to the channel estimation problem in MIMO-OFDM has been explained, which makes it easy to apply the same bit loading algorithms to both OFDM and MIMO-OFDM systems by decomposing the MIMO channel matrix into R parallel independent channels. The wireless channel model considered in this work and method of its generation has been shown. Also, provided are the examples of different time-varying correlated channels that have been employed in this work. Since quantization plays an important role in compressing the feedback, a brief explanation of quantization techniques and the various compression algorithms used in the simulation have been given. Run length encoding, Huffman coding and LZW compression algorithms have been used in this work, and their performances are compared based on the results achieved. Although, it is believed that Huffman is guaranteed to achieve best results when statistics are known, however, under the

constraint that each source message is mapped to a unique codeword and that the compressed text is the concatenation of the codewords for the source messages. The Lempel-Ziv code is not designed for any particular source but for a large class of sources. Surprisingly, for any fixed stationary and ergodic source, the Lempel-Ziv algorithm performs just as well as if it was designed for that source. Mainly for this reason, the Lempel-Ziv code is the most widely used technique for lossless file compression. The comparison results obtained in this thesis would prove how well these algorithms perform in case of the adaptive allocations. The next chapter deals with the bit loading algorithms used for optimal bit loading in adaptive multicarrier systems, and also, an analysis of the feedback data generated by using these bit loading algorithms is given. It also explains the related research work with regard to this thesis.

Chapter 3

Feedback in Adaptive OFDM and MIMO-OFDM Systems

3.1 Feedback Data Analysis

This section explains in detail about the bit loading algorithms used in OFDM and MIMO-OFDM systems, and the amount of feedback data generated in different conditions. Also, the related research has been described where methods for data reduction have been applied.

3.1.1 Adaptive Bit Allocation

The bit error probability for different OFDM subcarriers transmitted in time-dispersive channels depends on the frequency domain channel transfer function. The occurrence of bit errors is normally concentrated in a set of several faded subcarriers, while the other subcarriers will experience relatively lower bit errors. If the subcarriers that will exhibit high bit error probabilities in the OFDM symbol to be transmitted can be identified and excluded from data transmission, the

overall BER can be improved in exchange for a slight loss of system throughput. This is the motivation behind adaptive modulation.

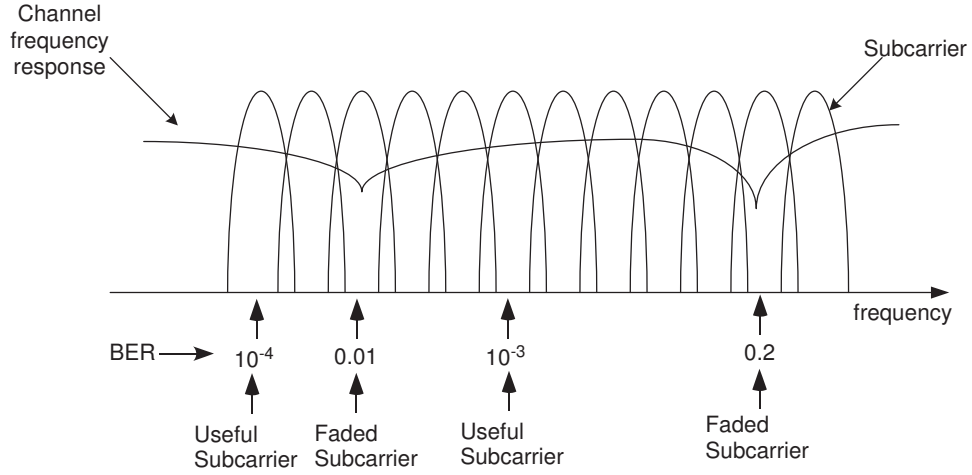


Figure 3.1. Different Subcarriers BER Performance Illustration

As the frequency domain fading deteriorates the SNR of certain subcarriers, but improves other subcarriers above the average SNR value, the potential loss of throughput due to the exclusion of faded subcarriers can be mitigated by employing higher order modulation modes on the subcarriers exhibiting high SNR values. Figure 3.1 illustrates the subcarriers performance. It can be seen that, due to fading in the channel, the subcarrier BER is affected and the faded subcarriers are excluded if necessary, to keep the overall system performance in good condition.

This estimation of future channel parameters for the purpose of adaptive modulation can be obtained by extrapolation of finite previous channel estimations, which are acquired upon detecting each received OFDM symbol. Therefore, the channel characteristics have to be slowly varying compared to the estimation interval [39]. In the context of time-varying channels, there is a decorrelation time associated with each frequency-selective channel instance. Thus, a new adapta-

tion must be implemented each time the channel decorrelates. Adaptation of the transmission parameters is based on the transmitters perception of the channel conditions in the forthcoming time-slot.

Adapting the transmission technique to the channel conditions on a time-slot by time-slot basis for serial modems in narrowband fading channels has been shown to considerably improve the BER performance [40]. The Doppler fading rate of the narrowband channel has a strong effect on the achievable system performance; if the fading is rapid, then the prediction of the channel conditions for the next transmit time-slot is inaccurate, and therefore, the wrong set of transmission parameters may be chosen.

Adaptive modulation is only suitable for duplex communication between two transceivers, since the transmission parameters have to be adapted using some form of twoway transmission in order to allow channel measurements and signalling to take place. Transmission parameter adaptation is a response of the transmitter to timevarying channel conditions. This is the purpose of feedforward and feedback channels.

In order to efficiently react to the changes in channel quality, the following steps have to be taken:

1. Channel quality estimation.
2. Choice of the appropriate parameters for the next transmission.
3. Signaling/blind detection of the employed parameters.

Channel Quality Estimation:

In order to appropriately select the transmission parameters to be employed for the next transmission, a reliable estimation of the channel transfer function during

the next active transmit time-slot is necessary. Since this knowledge can only be gained by prediction from the estimation of past channel quality, the adaptive system can only operate efficiently in an environment exhibiting relatively slowly varying channel conditions.

For OFDM modems, the bit error probability in each subcarrier is determined by the fluctuations of the channels' instantaneous frequency domain channel transfer function if no interference is present. The estimate of the channel transfer function can be acquired by means of pilot tone based channel estimation. More accurate measures of the channel transfer function can be gained by means of decision directed or time domain training sequence based techniques [41]. The estimate of the channel transfer function does not take into account effects such as cochannel or intersubcarrier interference. The delay between the channel quality estimation and the actual transmission of the OFDM symbol in relation to the maximal Doppler frequency of the channel is crucial with respect to the adaptive systems performance.

This thesis employs closed loop adaptation where the receiver has to estimate the channel quality and explicitly signal this perceived channel quality information to the transmitter in the reverse link.

Choice of the Appropriate Parameters for the Next Transmission:

Based on the prediction of the channel conditions for the next time-slot, the transmitter has to select the appropriate modulation modes for the subcarriers.

Different transmission parameters can be adapted to the anticipated channel conditions, such as the modulation schemes and coding rates. Based on the estimated frequency domain channel transfer function, spectral predistortion at the transmitter of one or both communicating stations can be invoked, in order to

partially or fully counteract the frequency selective fading of the timedispersive channel. In addition to improving the systems BER performance in timedispersive channels, spectral predistortion can be employed in order to perform all channel estimation and equalization functions at only one of the two communicating duplex transceivers.

Signaling or Blind Detection of the Employed Parameters:

The receiver has to be informed as to which demodulator parameters to employ for the received packet. This information can either be conveyed within the OFDM symbol itself, at the cost of loss of effective data throughput, or the receiver can attempt to estimate the parameters employed by the remote transmitter by means of blind detection mechanisms [42].

Signaling plays an important role in adaptive systems and the range of signaling options is open-loop and closed-loop signaling. If the channel quality estimation and parameter adaptation have been performed at the transmitter of a particular link, based on open-loop adaptation, then the resulting set of parameters has to be communicated to the receiver in order to successfully demodulate the OFDM symbol. If parameter adaptation is done at the receiver itself using the closedloop scenario, then the same amount of information has to be transmitted to the transmitter in the reverse link. If this signaling information is corrupted, then the receiver is generally unable to correctly decode the OFDM symbol corresponding to the incorrect signalling information. Efficient and reliable signalling techniques have to be employed for practical implementation of adaptive OFDM systems.

Figure 3.2 from [6], shows an MCM system employing the adaptive loading algorithm. As explained in earlier, this thesis considers the closed-loop adaptation.

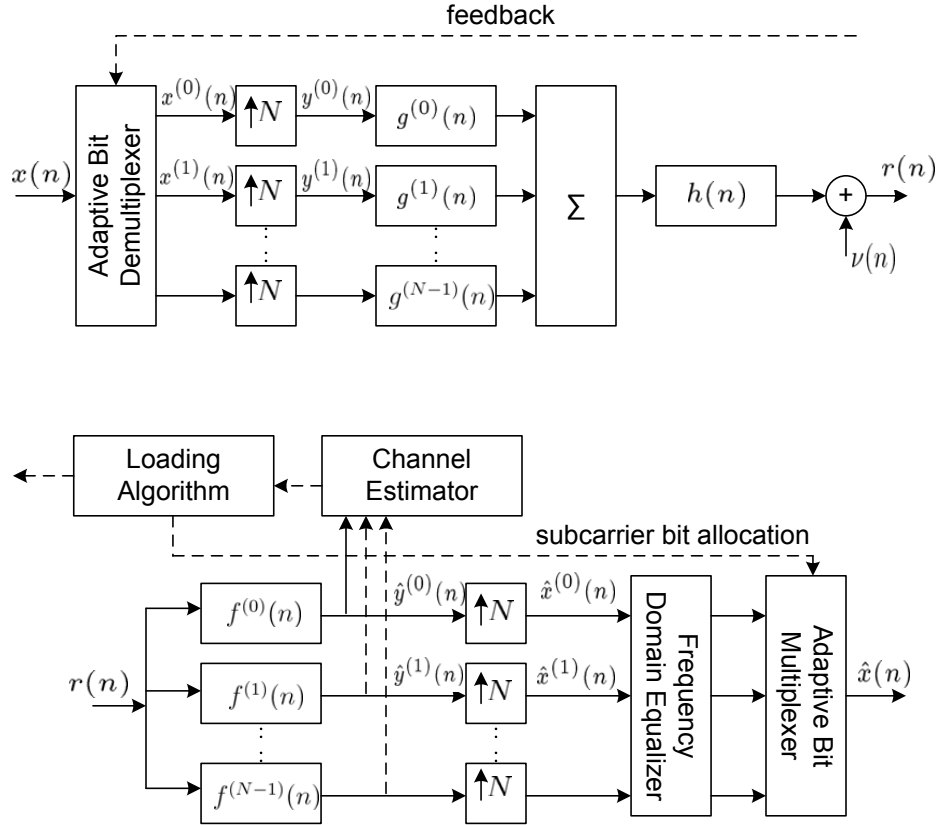


Figure 3.2. MCM Transmitter and Receiver With Adaptive Bit Loading Algorithm

With the help of channel estimation, new allocation parameters for adaptation are generated by the bit loading algorithm at the receiver and fed back to the transmitter through reverse link. It can be seen from the Figure 3.2, how the high speed input symbol stream is demultiplexed into N streams, each stream having varying bit allocation. After applying the IFFT operation, a composite signal is transmitted across the channel. The received signal is separated into N subcarriers using the FFT operation, equalized, demodulated and multiplexed together to form the estimate of actual input signal. The optimal adaptive transmission scheme, which achieves the Shannon capacity for a fixed transmit power, is the *waterfilling distribution* of power over the frequency-selective channel [43]. How-

ever, while the waterfilling distribution will indeed yield the optimal solution, it is difficult to compute and it tacitly assumes infinite granularity in the constellation size, which is not practically realizable.

The adaptive loading technique employed in this thesis is an efficient technique for achieving power and rate optimization based on knowledge of the subchannel gains [44, 45].

In the discrete bit loading algorithm of [44], we are given a set of N increasing convex functions $e_n(b)$ that represent the amount of energy necessary to transmit b bits on subcarrier n at the desired probability of error using a given coding scheme. We will assume $e_n(0) = 0$.

The allocation addressed in this thesis is an energy minimization procedure defined as:

$$\min \sum_{n=1}^N e_n b(n) \quad (3.1)$$

$$b_n \in \mathbb{Z}, b_n \geq 0, n = 1, 2, \dots, N, \text{ and} \quad (3.2)$$

$$\text{s.t. } \sum_{n=1}^N b_n = B. \quad (3.3)$$

To initialize the bit allocation, the scheme found in [45] was employed as shown in Figure 3.3.

SNR GAP (Γ) is a tuning parameter. Different values for Γ yield different Eb/No ratios for a given desired number of bits B to transmit. This is because the Γ directly impacts the energy table value calculations. Thus, tuning the Γ allows us to characterize the BER performance of the system.

Consider the k^{th} subcarrier. Given the channel gain and noise PSD, the energy increment table will provide the incremental energies required for the subcarrier data rate to transition from 0 bit to 1 bit, 1 bit to 2 bits, 2 bits to 3 bits, and so

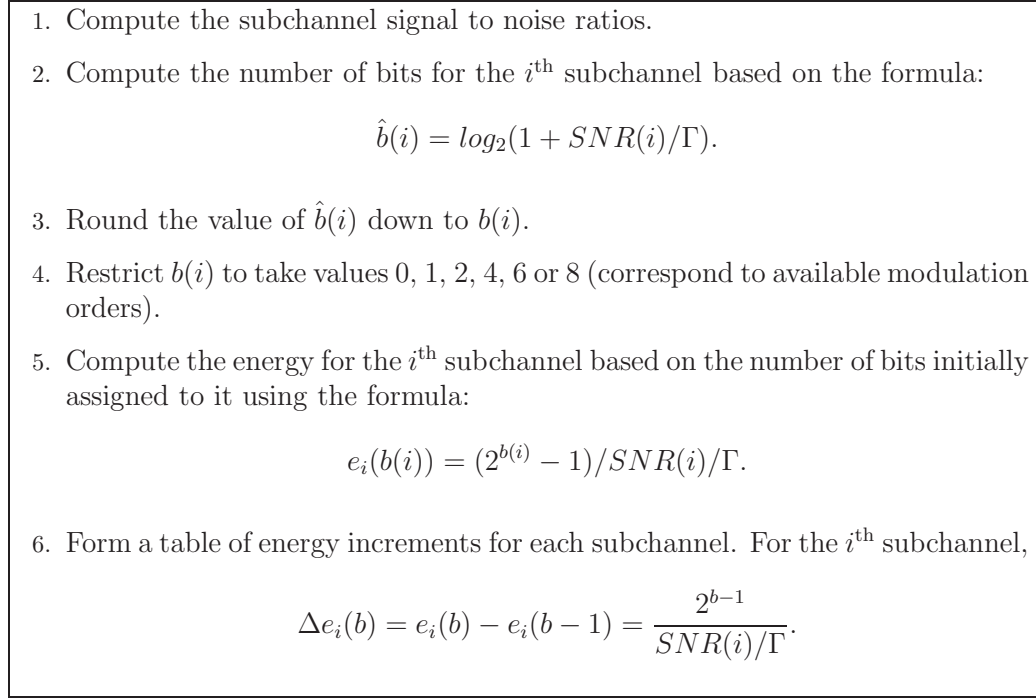


Figure 3.3. Chow's Bit Loading Algorithm

on. If only even numbered bits are to be used in the system, the energy increment table has to be changed using a clever averaging technique [44].

For example, suppose the energy increment required for supporting an additional bit from 2 bits in the n^{th} subcarrier is 30 Joules, and that required for supporting an additional bit from 3 bits is 40 Joules. Then, reassign the energy increment values to the same value, namely, the average of the two. In this case, that value is 35 Joules. This assures us that if a subcarrier is allocated a single bit for going from 2 bits to 3 bits, then in the next iteration the same minimum amount of additional energy required to support another bit implies that the same subcarrier will be allocated the next bit as well.

The same averaging procedure is repeated for all other possible bit transitions. The only exception that might arise is when the algorithm terminates, not having

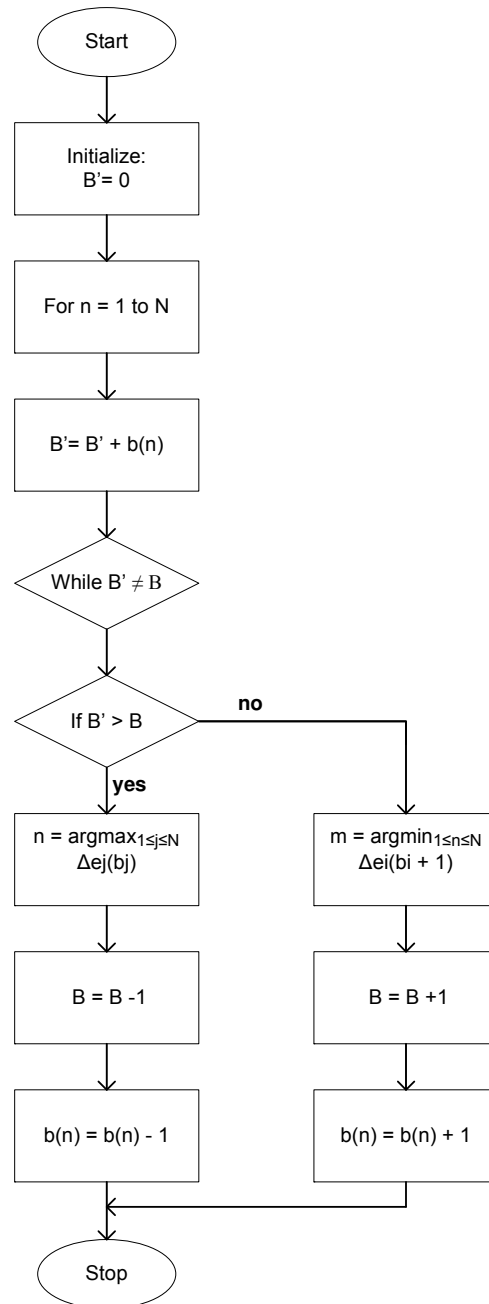


Figure 3.4. Flowchart Describing the Campello's Optimization Algorithm of Bit Allocation

assigned the final bit to even out the total number of bits on that subchannel. In order to resolve this issue, we used an algorithm proposed in [44], which will be discussed in the detail later in this section.

Given the initial bit allocation, the algorithm shown in Figure 3.4 optimizes the bit allocation, which is nothing but the B -tightness algorithm [44]. B -tightness simply guarantees that the fixed rate constraint in the discrete loading problem is met. A bit distribution \mathbf{b} with granularity β and total bits per symbol b is B -tight if $\mathbf{b} = \sum_{n=1}^N b_n$. The B -Tighten algorithm is the data rate preserving algorithm. Given any bit distribution, it iteratively subtracts a β bits when the total number of bits is greater than the limit and adds β bits when the total bit distribution exceeds the limit. This algorithm has a very simple stopping criterion. Combining the algorithms outlined, one can find the optimum solution to discrete bit loading problems by first efficientizing and then tightening a candidate solution. The speed of the convergence depends on the initial bit distribution. Since there is a restriction on the number of bits that each subcarrier can carry, the algorithms have been modified accordingly.

Finally, in order to deal with a single violated bit constraint, we employ the following algorithm shown in Figure 3.5 [44].

The reason we have this constraint is that all the other subchannels will have 2, 4, 6, or 8 bits and allocating a single bit to them will violate the bit constraint. With these three algorithms, we have a complete characterization of the bit loading procedure for a given frequency selective channel.

To demonstrate the bit and energy allocations, an instance of the channel was generated and the optimal bit allocation was found. Figure 3.6 shows the channel frequency response, the allocation of bits to each tone, and the corresponding

1. Check that the input bit allocation contains at most one violation of the bit constraint.
2. If there is a single violation, (say it is in subchannel ν), find the bit from the current bit allocation having the largest incremental energy that can be used to fill up subchannel ν . Let,

$$E1 = \Delta e_{\nu}(b(\nu)) - \Delta e_i(b(i)).$$

3. Find the bit that will cost the least to increment in the other subchannels which have been allocated either 0 or 1 bit only. Let,

$$E2 = \Delta e_j(b(j) + 1) - \Delta e_{\nu}(b(\nu)).$$

4. Perform the change corresponding to the smallest of E1 and E2.

Figure 3.5. Algorithm to Deal With Single Violated Bit Constraint

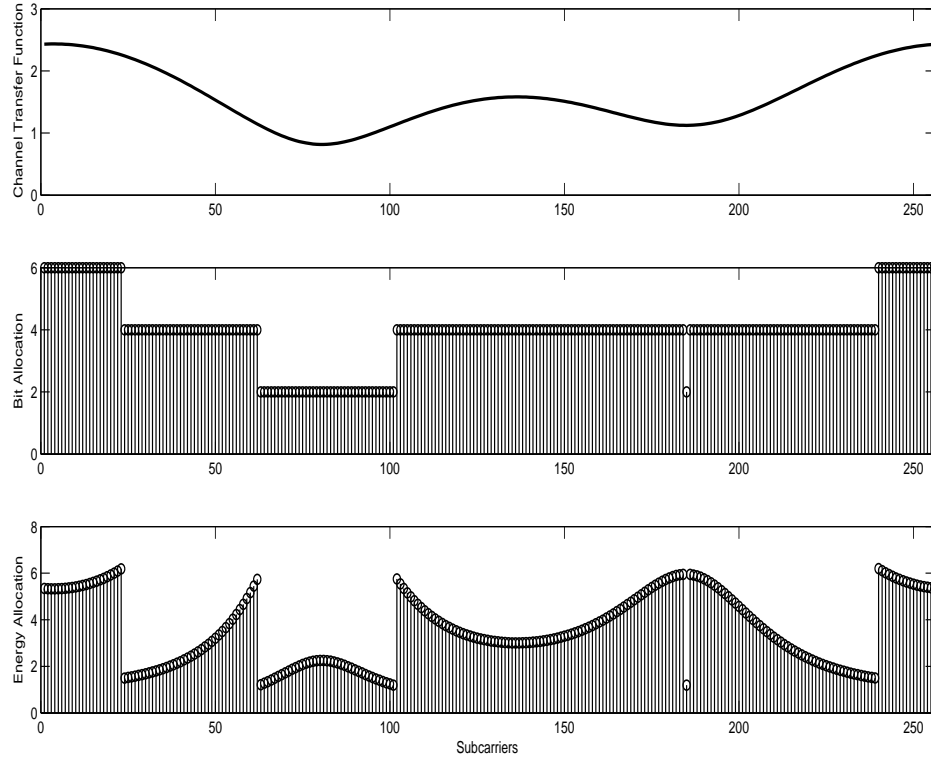


Figure 3.6. Energy and Bit Allocation for a Channel Instance

energy on each tone.

So, from Figure 3.6 we can see that the size of bit and energy allocations is directly proportional to number of subcarriers N . For transmitting the feedback data which is a combination of bit and energy allocation values, these values are converted to binary form, and total size would be approximately $2 * N * (b + e)$, where b represents the number of binary bits required to represent bit allocation values, and e represents the number of binary bits required to represent quantized energy allocation values.

3.2 Related Research

Large amounts of channel state information (CSI) feedback and signalling overhead can be a serious problem in adaptive OFDM and MIMO systems. Recent researchers have paid much attention to this problem.

In the context of bit loading for dynamic adaptation for point-to-point connections, two related studies have been published [14, 46]. Reference [46], aimed at highlighting two major issues dealing adaptive modulation based on bit loading algorithms. The first one is correlation due to Doppler in order to reduce the bit loading complexity, and the second is the signalling information related to the bit mapping structure. By applying the LZW source coding algorithm, the researchers could achieve reasonable compression.

Reference [14] addressed multicarrier systems whose link adaptation is carried out by means of bit loading algorithms. The associated signalling load increases quickly with the number of subcarriers, modulation schemes and users. These bit loading vectors are considered *a priori* known at the receiver. An adaptive loss-less compression system for an optimized compression performance and complexity is

proposed, based on run length encoding which was shown to be more suitable than the LZW algorithm. However, these studies do not consider the principal performance impact due to the signaling overhead. Instead, they focus on suitable compression schemes.

Reference [47] proposed using one bit channel state feedback for each subcarrier, and this one bit is used to indicate the subcarrier selection or threshold based power allocation, e.g., 1 for one power level and 0 for another. This method provides very limited adaptive capability and works well for excluding deep faded subcarriers. As compared to the subcarrier-to-subcarrier adaptation mode, i.e. each subcarrier with one independent adaptation mode and signalling loop, grouping is proved to be effective in reducing transceiver complexity, CSI feedback and signalling overhead, since the same adaptive mode will be used in all member subcarriers of a group instead of one mode for one subcarrier. Besides, only minor modifications of traditional adaptive techniques need to be done for transmissions based on this kind of feedback.

Reference [48] has proposed a grouping adaptive modulation OFDM system, which separates subcarriers into groups for the same modulation. Reference [49] proposed to process subband bit and power loading based on grouping the subcarriers according to the ascending order of subcarrier channel gains. Reference [50] focused on practical feedback and adaptive signalling designs of OFDM systems. Based on the investigations of the characteristics of frequency-selective channels, the Dynamic Neighboring Subcarrier Grouping Scheme (DNSGS) is proposed to cut down the feedback and adaptive signalling overhead, and to simplify the implementation of OFDM adaptive techniques. The simulation results show that DNSGS is flexible enough for different kinds of communication environments, and

can effectively cut down the feedback and signalling overhead with rather limited performance penalty. Besides, DNSGS outperforms the existing grouping schemes greatly.

However, these methods either do not consider the characteristics of transmission channels or do not effectively cut down the adaptive signalling overhead.

3.3 Chapter Summary

In this chapter, bit loading algorithms employed in this work are explained in detail. Also, the result of applying the algorithms to our adaptive OFDM system and feedback data, i.e., bit and energy allocations generated based on the channel conditions, has been shown. An analysis of the average size of feedback data being generated in our simulation system has also been explained in detail. A brief explanation of the related research work has also been given in this chapter. Now, our system is effectively generating bit and energy allocations using the bit loading algorithms for time-varying channel conditions. The next chapter deals with the feedback reduction scheme employed in this work, which exploits the time-correlation properties and helps in reducing the number of feedback transmissions. The results explaining the compression achieved by using compression algorithms along with the feedback reduction scheme have been explained in detail.

Chapter 4

Feedback Compression in Adaptive OFDM and MIMO-OFDM Systems

This section explains the feedback reduction scheme, the methods employed for compression of the feedback data, and the results achieved. Also, the relation between the number of quantization levels and the reduction and compression ratio has been explained.

4.1 Feedback Reduction Scheme

This section talks in detail about the approach used for reducing the feedback data in adaptive wireless multicarrier systems. In any general adaptive OFDM and MIMO-OFDM system, a new set of allocation parameters are fed back for each time-varying channel instance so that the system adapts effectively to the time-varying channel condition. Thus, the number of times feedback is transmitted

depends on the length of the time-varying channel and on the time correlation between each channel instance. The main motivation of this thesis is to reduce the number of times the feedback data has to be transmitted, and to achieve a reasonable compression using suitable compression schemes. As the feedback transmissions also vary depending on the type of time-varying channel, several channel correlations, such as slow varying to very fast varying channels have been considered in this thesis. For reducing the number of feedback transmissions, we have employed a scheme as described.

Figure 4.1, is a general schematic of the feedback reduction scheme. As shown, the system starts with initial bit and energy allocation values for the first channel instance. Then, the data bits are spread onto the $N = 256$ subcarriers using modulation techniques and IFFT. Then, the data pass through the time-varying Rayleigh fading channel, which is a combination of several channel instances having certain correlation with each other, and the data are gathered back at the receiver using FFT and demodulation techniques. Here, the channel conditions are estimated and the system performance is measured by calculating the individual BER on each channel instance.

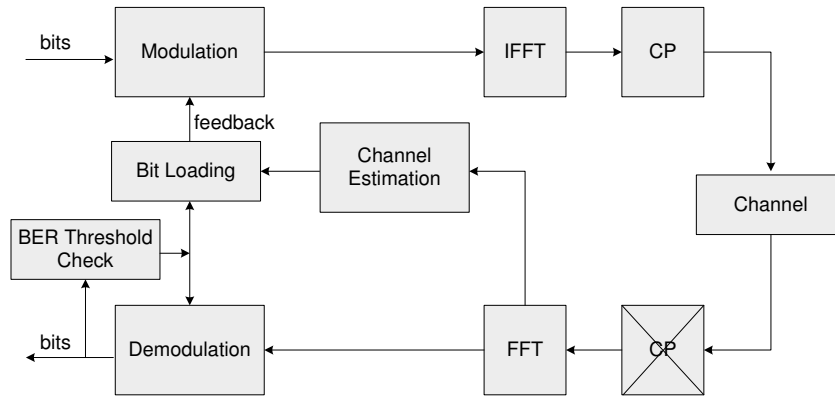


Figure 4.1. General OFDM Schematic Employing Feedback Reduction Scheme

In adaptive OFDM and MIMO systems, as soon as the channel conditions are estimated, a new set of allocation values are generated and fed back to the transmitter to adapt according to the channel conditions. Suppose there are C time varying channel instances; for each channel instance the feedback has to be transmitted, so the total feedback bits is $C * 2 * N * (b + e)$, where b and e represent the number of binary bits required to represent bit and quantized energy allocations which would obviously occupy a reasonable amount of the bandwidth. This feedback is transmitted even when the channel is slowly varying, where in such cases, the allocation values have only very slight differences with each other. This approach concentrates on taking advantage of such situations and reducing the number of feedback transmissions of the allocations. The transmitter can be designed in such a way that if it receives any allocations through feedback, it employs them for the next transmission or it continues transmitting with the old allocation values. The threshold check box in Figure 4.1 checks if the mean BER value has crossed the threshold value and decides on providing the transmitter with a new set of bit and energy allocations or letting it continue with old allocation values.

Shown in Figure 4.2 is the flowchart describing the simulation setup of feedback reduction scheme in step-by-step manner. First a time-varying channel of length 100 instances is generated with a particular channel correlation value as described in Chapter 2. An initial bit and energy allocation values to be employed in the transmission are given by Chow and Campello's algorithm as described in Chapter 3. The OFDM system starts transmitting the data with these initial allocation values. At the receiver end, the data is received and the BER of each channel instance is calculated.

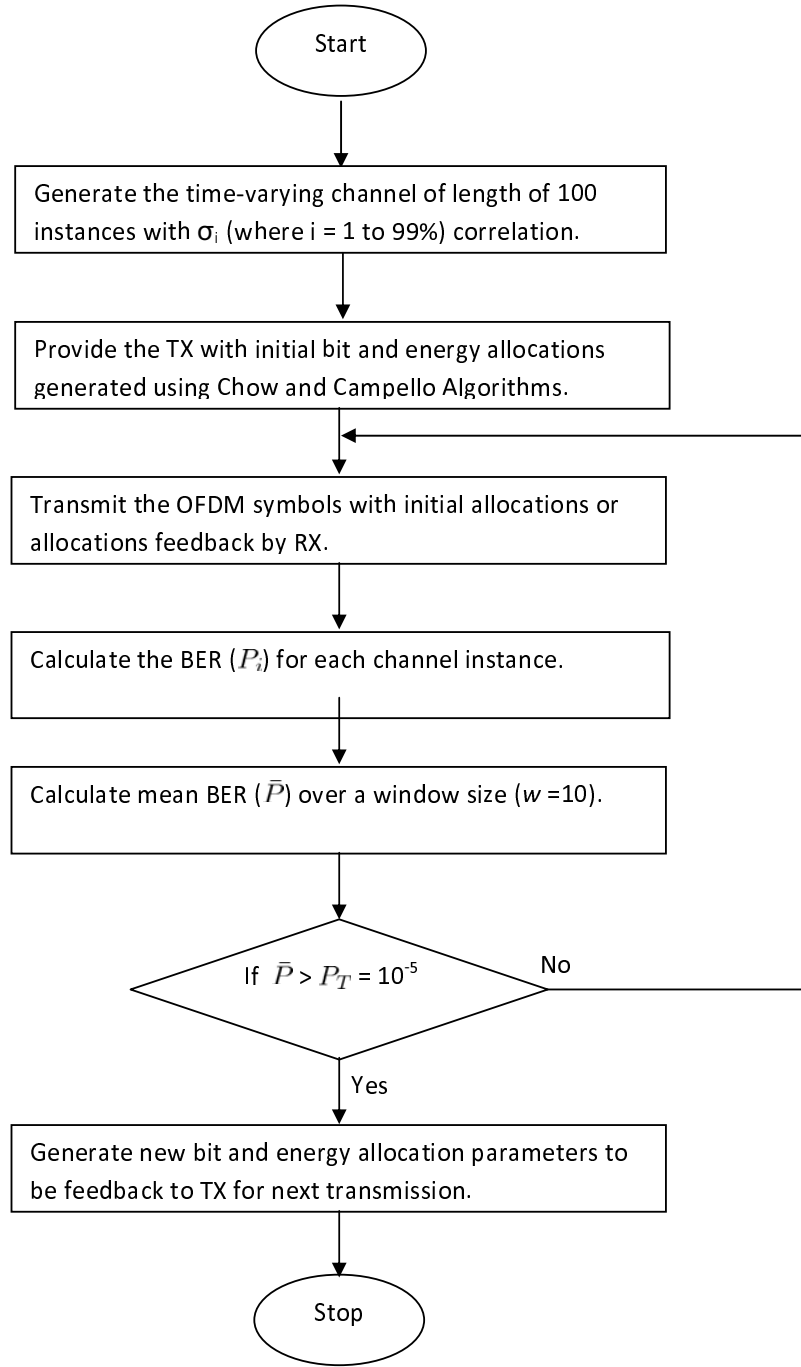


Figure 4.2. Description of the Feedback Reduction Scheme for Feedback Transmission Reduction in Adaptive Multicarrier Systems With Channel Correlations varying from 1% to 99%.

After calculating the BER P_i for each channel instance, the mean of BER (\bar{P}) values over a length of user defined window size (w) is compared to the threshold value $P_T = 10^{-5}$. If the value of \bar{P} crosses the threshold value P_T , then a new set of bit and energy allocations is generated and fed back to the transmitter; this new loading information is used for the next transmission. As long as \bar{P} stays below the threshold value, the transmitter uses only old allocation values for transmission and there is no need for feedback transmission. So, the number of feedback transmissions is reduced. This approach saves significant amount of bandwidth when employed in slowly time-varying channels, thus being able to concentrate on sending more data forward rather than wasting resources on feedback. How often we need to reconfigure the allocation values and feed back, depends on the channel correlations.

For the MIMO-OFDM case, as soon as time-varying channel is generated, each subchannel is decomposed into the frequency domain. The parallel decomposition of the channel is obtained by defining a transformation on the channel input and output through transmitter precoding and receiver shaping. The transmitter precoding and receiver shaping transform the MIMO channel into R_H (rank of channel gain matrix H) parallel single-input single-output (SISO) channels. Based on the number of transmitter and receivers employed (2 and 4 in our case), the system is given a set of initial bit and energy allocations to start the transmission. The same procedure described in the above paragraph is followed and the number of feedback transmissions for MIMO-OFDM 2×2 and MIMO-OFDM 4×4 are noted basing on the threshold check of BER values.

Whenever the \bar{P} crosses the threshold and new allocations are generated, a parameter, *number of feedback transmissions*, is incremented and this value tells

us the number of times feedback has been sent for this particular channel correlation. This is done for several channel correlation values, ranging from uncorrelated (1%) to highly correlated (99%) and the reduction ratio achieved by the feedback reduction scheme is compared to the unreduced feedback data. The results obtained describing the number of feedback transmissions and the reduced feedback ratio for OFDM and MIMO-OFDM are shown in the results section.

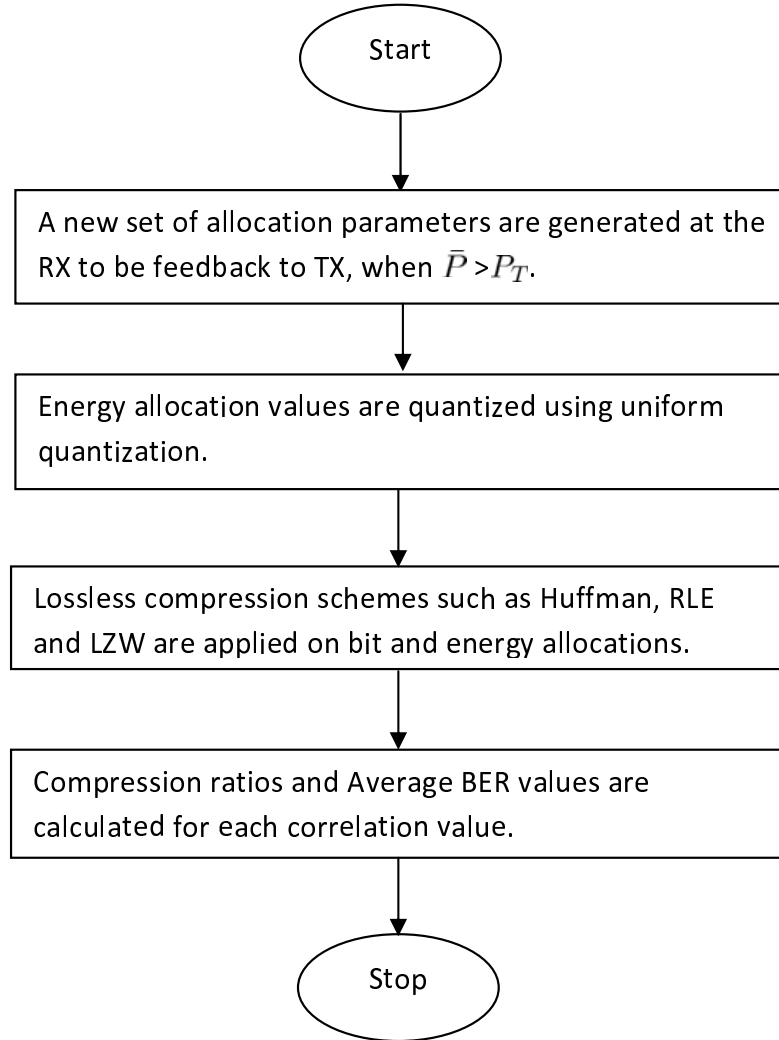


Figure 4.3. Description of Feedback Data Compression Methods Employed to Compress the Reduced Feedback Data in Adaptive Multicarrier Systems With Channel Correlations varying from 1% to 99%.

The feedback reduction scheme focuses on reducing the number of feedback transmissions, and the remaining part of this thesis deals with compression of this reduced feedback data using lossless compression algorithms and their comparisons. The method employed to compress the reduced feedback data effectively is shown in a step-by-step manner in Figure 4.3.

Since this part of the thesis becomes important only when \bar{P} has crossed the threshold value P_T and new allocations have been configured based on the channel condition and fed back, the description in the flowchart begins at that stage. The feedback data, as we know, is a combination of bits and energy allocation values. The energy allocation values are to be quantized before transmitting the feedback data, and this thesis employed a uniform quantization technique for quantization. OFDM and MIMO-OFDM system performance has been observed for various quantization levels.

Various lossless compression algorithms have been applied on the bit and quantized energy allocations to achieve compression. The most suitable compression algorithms that could be used in this case were Huffman coding, Run Length Encoding and LZW as explained in Chapter 2. The compressed feedback bits were fed back to the transmitter whenever the threshold check was positive. These bits are decompressed at the transmitter and the information is used for adaptively modulating the symbols for the next transmission. Also, the mean average BER of the systems for each type of channel correlation has been calculated for different quantization levels in order to understand the effect of lower quantization levels on the system performance. The compression ratios achieved using different compression schemes and the relation between mean average BER of the system and quantization levels are explained in the results section.

4.2 Simulation Results and Comparison

4.2.1 Simulation Parameters

All the simulations used 51200 bits, assuming 1024 bits transmitted in each of 50 transmissions per single channel instance. There are a total of 100 channel instances, and the number of symbols on each channel instance would vary depending on the adaptive allocations. So, the total number of transmitted bits over all the 100 time-varying channel instances is equal to 5120000. To ensure a fair comparison between OFDM and MIMO-OFDM systems, the total number of bits per single channel instance was kept constant. Generally, for a single transmission, as we can see from Figure 3.6, there would be N values each of bit and quantized energy allocations to be fed back proportional to the number of subcarriers $N=256$. Since we are considering 100 time-varying channels, there are 100×256 values to be converted to binary digits before transmission. As the number of subcarriers or as the number of channel time instances to be considered increases, the feedback data size automatically increases to a higher value.

The modulation scheme was chosen from the set of binary phase shift keying (BPSK), quadrature phase shift keying (QPSK), 16-level quadrature amplitude modulation (16-QAM), 64-QAM, 256-QAM, as well as “No transmission,” for which no signal was transmitted. These modulation schemes are denoted by M_m , where $m \in (0, 1, 2, 4, 6, 8)$ is the number of data bits associated with a subcarrier. Only six different square MQAM signal constellations are used; this scheme is expected to perform with an efficiency very close to that obtained by using unrestricted constellations [18]. Since we require our system to have a maximum of 8 bits, the energy increment required to go from 8 bits to 9 bits is set to a very high value.

Figure 4.4 is an example of the feedback data size of a normal OFDM and MIMO-OFDM systems. Feedback bits in a system for a particular channel correlation is defined as: number of channel instances $\times N \times$ binary representation of bit and energy allocations \times number of antennas employed. The feedback data size shown in the figure is defined as the feedback bits divided by the total transmitted bits, where the total transmitted bits as described in the simulation parameters, remained constant for all systems. As explained earlier, each channel instance is Rayleigh frequency-selective fading channel.

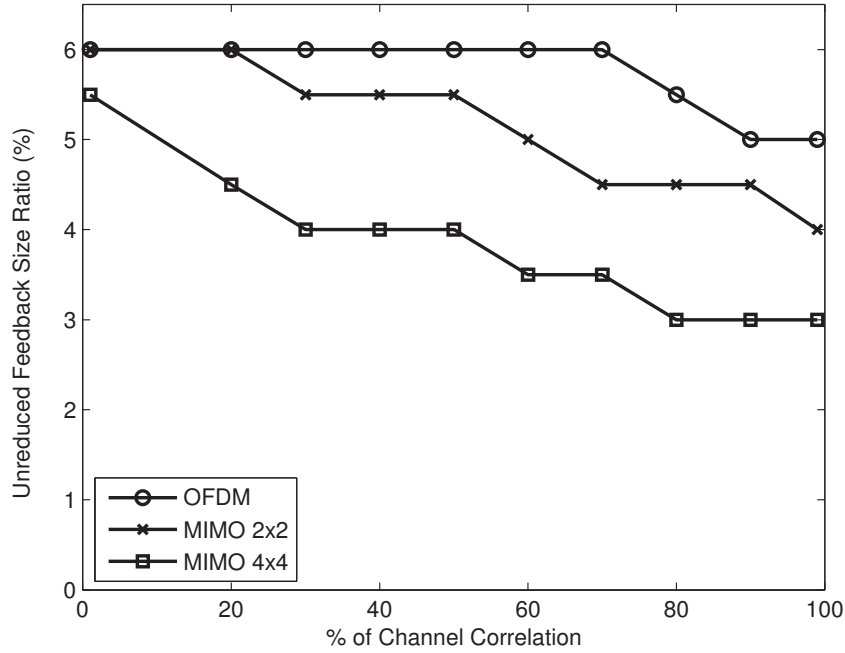


Figure 4.4. Feedback Size Ratio of a Normal OFDM and MIMO-OFDM Systems for Different Channel Correlations. Total Transmitted Bits = 5120000.

We have considered 10 different channel correlation values and calculated the feedback data size when no special techniques are applied to the system. We can see that the feedback size is high when the channel is varying faster, and is low

when its slowly varying channel. So, feedback size depends on the channel correlation and how fast it is varying. The trend observed in the graph is mainly due to the high energy allocation values for lower channel correlations. All the bit allocation values are represented by 3 binary bits and this binary bits are constant in all cases. When the system has a time-varying channel with lower channel correlation, there is a high fluctuation in the bit allocation information. Larger changes require higher energies for transmission, making energy allocation values higher. Thus, the total number of binary bits required for feedback data transmission is also high, as energy allocation value is the deciding factor in feedback data size. Varying quantization levels have been used to represent different ranges of the energy values to compare it with the performance of fixed quantization values. For higher channel correlations, the changes in the bit allocation values will be lower. Thus, the energy required to transmit these changes will also be low and the feedback data size is lower. We can see a trend when the correlation value is higher, i.e., as the channel becomes a slow time-varying channel, the maximum value of energy allocation decreases, and the total number of bits, thus results in a falling curve.

The OFDM feedback data size curve in Figure 4.4 starts to decrease only after 70% channel correlation, which implies that the system had the same maximum value of energy allocation in those channel correlations. After 70% channel correlation, the energy allocation values decreased, which made the curve decrease gradually. MIMO-OFDM systems experienced decreasing energy values for every other channel correlation which made the curve look like steps. MIMO-OFDM 4×4 had a lower feedback transmission size when compared to other two systems. The reduced feedback data achieved using the feedback reduction scheme and

the compressed feedback data achieved using compression algorithms have been compared with this unreduced feedback data.

4.2.2 Results

This section explains in detail all the results achieved for OFDM and MIMO-OFDM systems using the feedback reduction scheme and various compression algorithms. The MATLAB coding for this simulation has been written in such a way that the SISO case occurs as a special case of a MIMO system.

4.2.2.1 Feedback Reduction Scheme Results in OFDM and MIMO-OFDM Systems

When the feedback reduction scheme is applied to the OFDM and MIMO-OFDM systems as described, there is a constant check on the BER values of the system for each channel instance. The system performs well with the initial allocations, but as the channel slowly varies, the initial allocations are not effective past certain point. The BER values of the system worsen, which enables the threshold check to allow a new set of allocation parameters to be fed back to transmitter. When the time channel variation is fast, the initial allocations don't adapt to the conditions and therefore worsen the system performance in terms of BER, thus possibly requiring a greater number of feedback transmissions than slow varying channels. The effects of the feedback reduction scheme on the BER values of OFDM and MIMO-OFDM system are shown in the next few figures which explain the system performance when the channel is highly correlated, i.e., very slow varying. Figure 4.5 is a BER curve of an OFDM system when SNR=15dB and the channel correlation is 99%. These BER values have been

calculated for each channel instance. We can see that, as the same old allocations are being used initially, slowly the BER values rise and reach 10^{-5} , as a result, immediately the allocations are reconfigured and new set of values are fed back to the transmitter. So, the BER value immediately drops and then starts to rise again after transmission through certain channel instances. In this case we had to transmit the feedback data only 2 times instead of 100 times as in the general case.

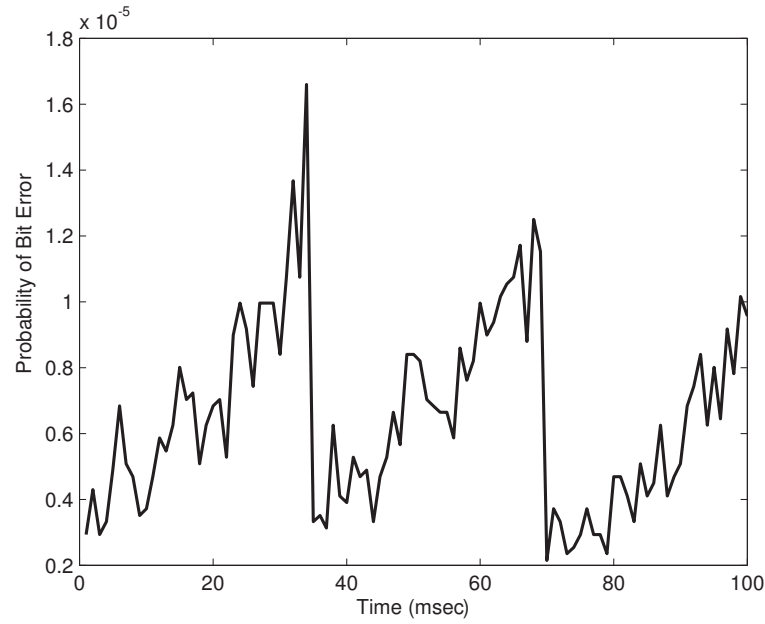


Figure 4.5. BER of Individual Channel Instances of an OFDM System for 99% Correlated Channel at SNR=15dB.

Figures 4.6 and 4.7 are the BER curves of individual channel instances of MIMO-OFDM systems with 2×2 and 4×4 transmitter/receiver configurations. MIMO-OFDM systems perform in the same way as an OFDM system, crossing the threshold only 2–3 times. These crossings of thresholds, which is nothing but the number of feedback transmissions, have been calculated for OFDM and MIMO-OFDM systems and shown in Figure 4.8 where we can see how many times

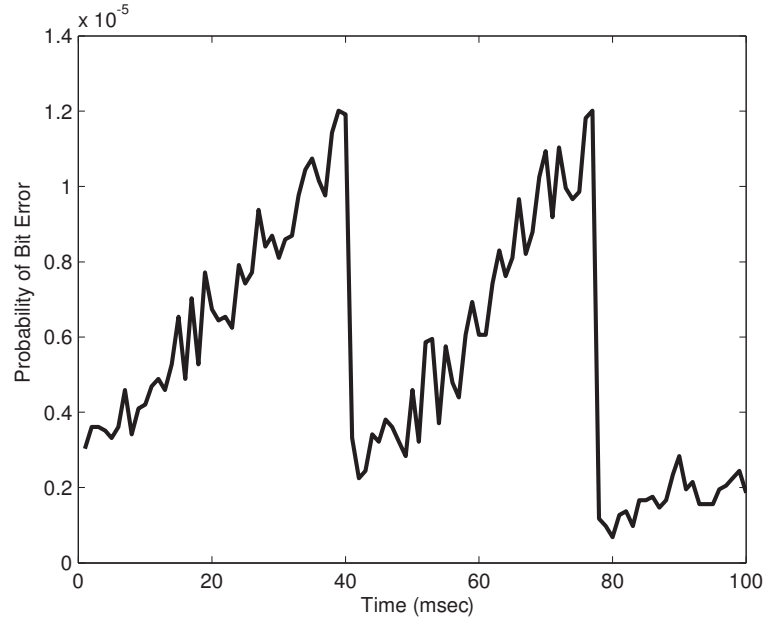


Figure 4.6. BER of Individual Channel Instances of a MIMO 2x2 System for 99% Correlated Channel at SNR=15dB.

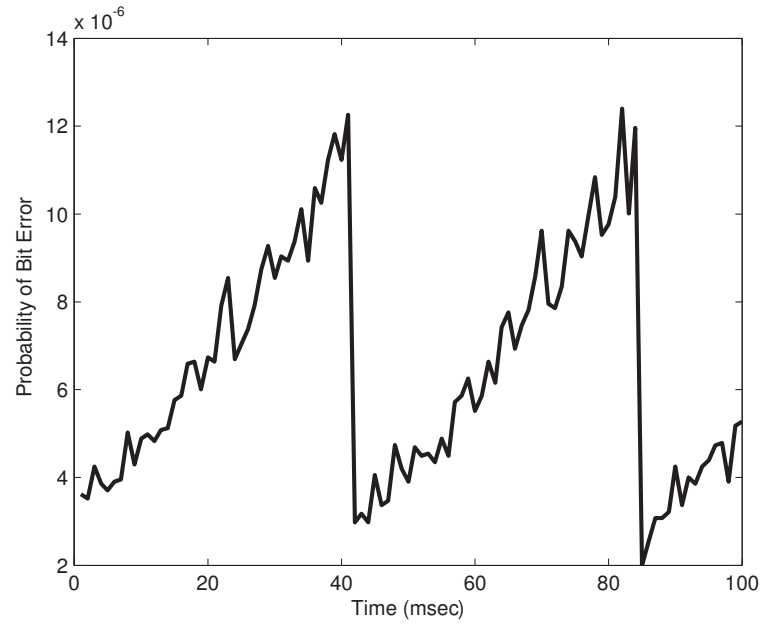


Figure 4.7. BER of Individual Channel Instances of a MIMO 4x4 System for 99% Correlated Channel at SNR=15dB.

a system has transmitted the feedback data for a particular channel correlation value.

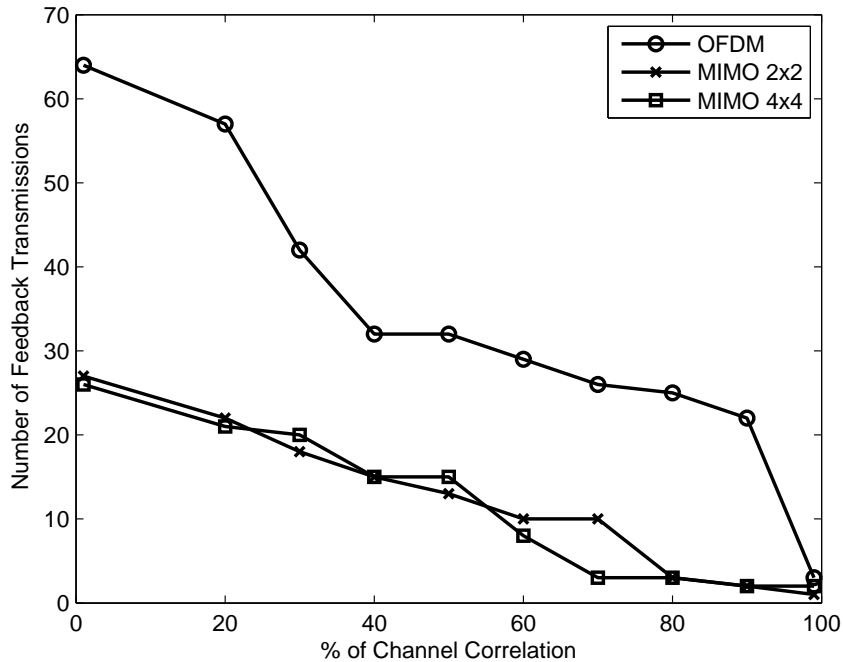


Figure 4.8. Reduction in Number of Feedback Transmissions Achieved Using Feedback Reduction Scheme in OFDM and MIMO-OFDM Systems.

Figure 4.8 shows the reduced number of feedback transmissions achieved using the feedback reduction scheme in OFDM and MIMO-OFDM systems. The threshold check on the BER is done only after the data has passed through 10 time-varying channel instances, since that is the user defined window size w . When the channel has high correlation, initial allocations being used for the next 10 transmissions affects the error rate negligibly. As described earlier, we had to transmit the feedback only 3 times for 99% channel correlation, which explains the lower feedback transmissions for higher channel correlations. When the channel has lower channel correlation, the error rate is effected badly, as previous

allocation information is not suitable for newer transmissions. So, the number of feedback transmissions gradually rise as the channel correlation decreases. We can observe that the highest number of times the feedback had to be transmitted in an OFDM system was 64 for a completely uncorrelated time-varying channel and only 3 times for a highly correlated channel. MIMO-OFDM 2×2 and MIMO-OFDM 4×4 system had same highest number of feedback transmissions, 28 and least, 3. We can clearly see that the MIMO-OFDM systems had a lower number of feedback transmissions compared to OFDM as they are more robust and perform better. We would have been required to send feedback data 100 times for every correlation value, if we did not use the feedback reduction scheme. All these results clearly demonstrate the advantages of this scheme. Results shown here have been simulated using varying bits per sample for representing quantization levels of energy allocations compared to the performance of fixed quantization levels.

Figure 4.9 shows the relation between the average BER values over all the subcarriers and different channel correlation values of OFDM and MIMO-OFDM systems. We can see that while using the feedback reduction scheme, the average BER values are less for higher channel correlation values, but as the correlation between channel instances decreases, the average BER tends to rise. This is because of the system using old allocation values until the BER values of individual channel instances over a window size length cross the threshold. But as the channel correlation decreases, there is a need for providing the transmitter with newer allocations with greater speeds. But in our case there is a delay occurring in sending the feedback to satisfy the threshold condition as described in the reduction scheme, and this is the reason the average BER values of the overall system keep rising with the decrease of channel correlation values. As seen in the

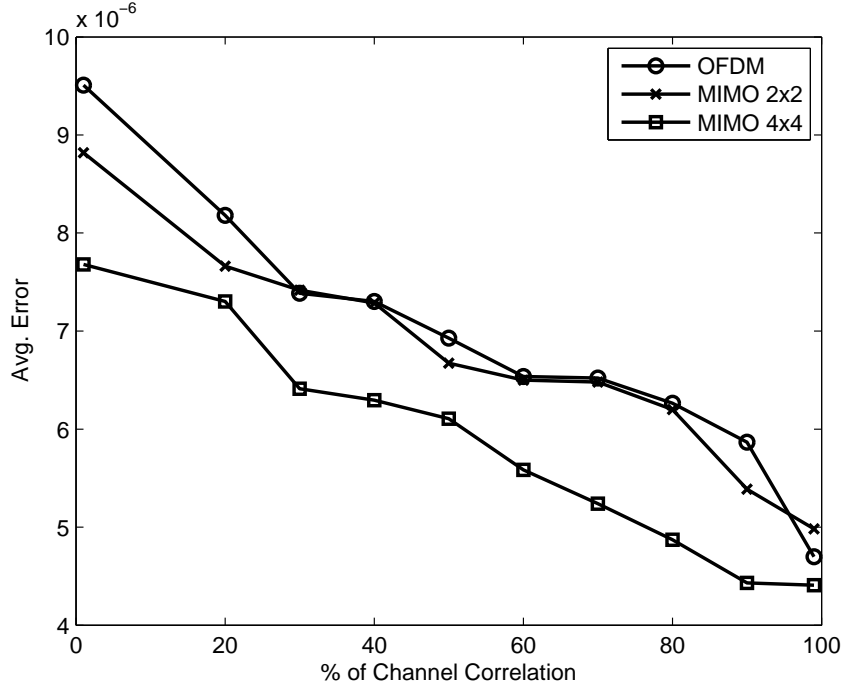


Figure 4.9. Average BER Value Curves of OFDM and MIMO-OFDM Systems for Various Channel Correlations.

figure, the MIMO-OFDM 4×4 performs better than the other two cases considered here.

Shown in Figure 4.10 is the graph of reduced feedback data size achieved by using the feedback reduction scheme in OFDM and MIMO-OFDM systems. Also shown in the same figure in dotted lines is the case of unreduced feedback size i.e., Figure 4.4 for a comparison purpose. Here the feedback data is defined as: number of feedback transmissions $\times N \times$ binary representation of bit and energy allocations \times number of antennas employed. So the number of feedback transmissions decide the size of feedback data when the reduction scheme is applied to the system. As explained, the total number of transmitted bits over all the 100 time-varying channel instances is constant equal to 5120000. The OFDM system could achieve an average reduction ratio of 66.52% over all channel correlations.

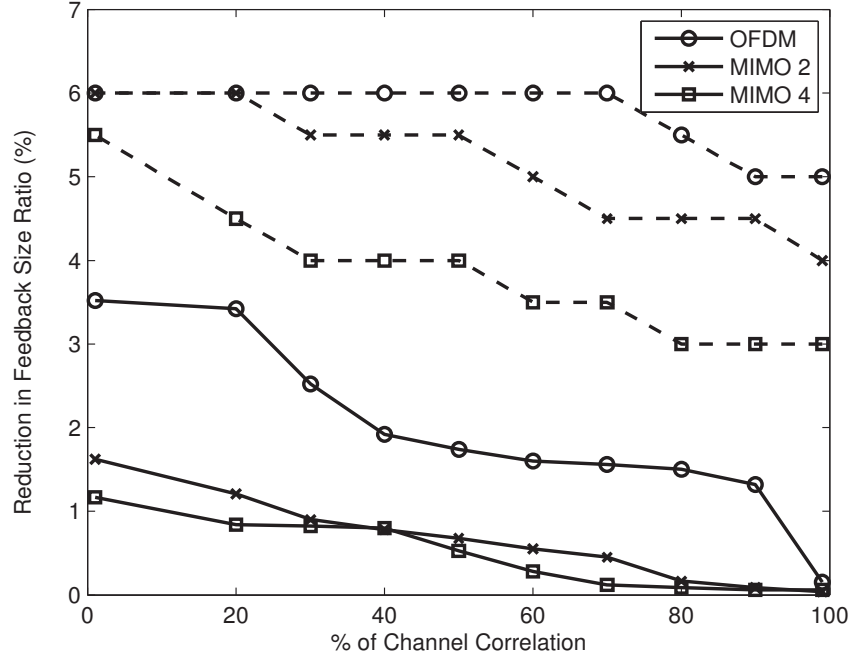


Figure 4.10. Reduction in Feedback Size Ratio Achieved Using the Feedback Reduction Scheme in OFDM and MIMO-OFDM Systems. Solid Lines for Reduced Feedback and Dotted Lines for Unreduced Feedback. Total Transmitted Bits = 5120000.

It could achieve a 97% reduction in the feedback data size for high channel correlation when compared to the unreduced case. This makes sense when we compare the graphs of unreduced and reduced cases. The number of feedback transmissions in the unreduced case was 100 and only 3 in the reduced case, which made the system achieve 97% reduction in the feedback data, the least reduction being 36% for no channel correlation. MIMO-OFDM 2×2 achieved an average reduction of 87.29% by using this feedback reduction scheme, the highest reduction being 97% for high channel correlation and the least being 73% for no channel correlation. MIMO-OFDM 4×4 achieved an average reduction of 87.44% using the reduction scheme, the highest reduction ratio being 97% for high channel correlation and the least being 74% for no channel correlation. Both configurations

of MIMO-OFDM systems achieve an almost equal feedback reduction ratio while outperforming the OFDM system by achieving 24% more reduction. By applying this reduction scheme to the OFDM and MIMO-OFDM systems, a reasonable reduction in the number of feedback transmissions and thus the feedback data size has been achieved.

In this section we have shown various system performance enhancements achieved by employing the feedback reduction scheme. The results clearly show the effectiveness of the scheme in taking advantage of time-correlation present in the wireless channels and helping systems reduce the number of feedback transmissions and the feedback data. The next section deals with the results obtained when different lossless compression algorithms are applied to this reduced feedback data.

4.2.2.2 Quantization and Compression Results in OFDM and MIMO-OFDM Systems

One of the more common and simpler examples of lossless compressions, run length encoding, is applied first to the feedback data achieved after applying the reduced feedback scheme to the system. Figure 4.11 shows the compression ratio achieved from the reduced feedback data in a OFDM and MIMO-OFDM system using Run Length Encoding (RLE) compression. Shown in the same figure in dotted lines is the uncompressed case to which the comparison has been done and compression ratios have been calculated. Compression ratio is defined as the feedback data in the compressed case divided by the feedback data in the unreduced case. Since our main aim in this thesis is to talk about how much the unreduced feedback can be compressed, the comparison has been done with the unreduced case rather than reduced case. As explained, the total number of transmitted bits

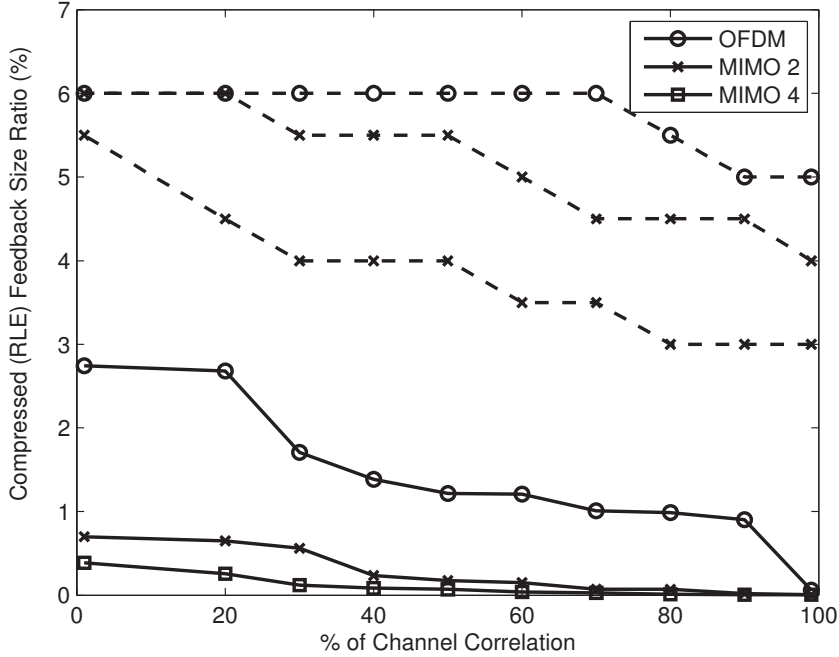


Figure 4.11. Compression of Feedback Size Ratio Achieved in OFDM and MIMO-OFDM Systems Using Run Length Coding. Solid Lines for Compressed Feedback and Dotted Lines for Unreduced Feedback. Total Transmitted Bits = 5120000.

over all the 100 time-varying channel instances is constant and equal to 5120000 for all the cases where compression algorithms have been applied. RLE compression as described replaces any repetitions of the same bit or byte that occur in a sequence of data with a single occurrence of the bit/byte and a run count. Our bit allocations have a lot of redundancy, as there are only six modulation schemes being considered, and also there is good amount of redundancy introduced into the energy allocations due to the quantization. When the RLE compression algorithm was applied to the reduced feedback data achieved from the feedback reduction scheme, we could achieve an average compression ratio of 75% in the OFDM system, 90.3% in the MIMO-OFDM 2×2 and 90.7% in the MIMO-OFDM 4×4 system. The OFDM system could achieve an individual compression ratio

of 98% for highly correlated channel and 51% compression for uncorrelated channel. MIMO-OFDM 2×2 could achieve an individual compression of 98% for high correlated channel and 80% for uncorrelated channel. MIMO-OFDM 4×4 could achieve an individual compression of 98% for highly correlated channel and 82% for uncorrelated channel. MIMO-OFDM 2×2 and MIMO-OFDM 4×4 performed equally and they both achieved 15% more compression than the OFDM system when RLE compression was considered. RLE, even though being such a simple lossless compression algorithm, when combined with the feedback reduction scheme, could achieve a significant compression on the feedback data.

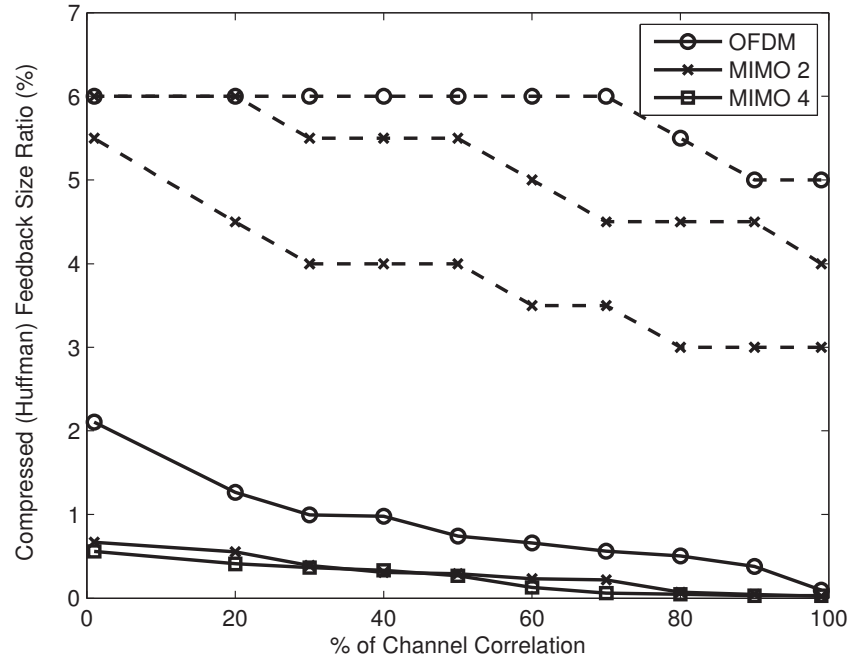


Figure 4.12. Compression of Feedback Size Ratio Achieved in OFDM and MIMO-OFDM Systems Using Huffman Coding. Solid Lines for Compressed Feedback and Dotted Lines for Unreduced Feedback. Total Transmitted Bits = 5120000.

Huffman compression, also known as Huffman encoding, is one of many and one of the most famous compression techniques in use today. The Huffman com-

pression algorithm assumes data files consist of some symbol values that occur more frequently than other symbol values in the same file. The most common characters in the input file (i.e., characters with higher probabilities) are assigned short binary codes. Least common characters (i.e., with lower probabilities) are assigned longer binary codes. Shown are the results achieved when the Huffman coding is applied to the feedback data. Figure 4.12 shows the compression ratios achieved on the reduced feedback data in OFDM and MIMO-OFDM systems using Huffman coding. Shown in the same figure in dotted lines is the uncompressed case to which the comparison has been done and compression ratios have been calculated. When Huffman coding was applied to the reduced feedback data, a compression ratio of 85.5% was achieved in the OFDM system, 94.7% in MIMO-OFDM 2×2 and 94.6% in MIMO-OFDM 4×4 systems. OFDM could achieve a compression of 98% for highly correlated channel and 61% for uncorrelated channel. MIMO-OFDM 2×2 could achieve a compression of 98% for highly correlated channel and 88% for uncorrelated channel and MIMO-OFDM 4×4 could achieve a compression of 98% for high channel correlation, 87% for no channel correlation. MIMO-OFDM 2×2 and MIMO-OFDM 4×4 performed equally and they both achieved 9% more compression than OFDM when Huffman coding was considered. Huffman coding when employed along with the feedback reduction scheme, could achieve a very high compression ratio and it outperformed the RLE compression algorithm in OFDM by 10% more compression and in MIMO-OFDM systems by 4% more compression. This implied that the feedback data consisted of a greater number of frequently occurring symbols which helped Huffman coding perform better than RLE. When the channel correlation is high, the individual compression ratios achieved by both RLE and Huffman remain the same but the

when the channel correlation is low, Huffman coding could achieve higher compression ratios since this is based on probability of occupancy rather than repetition in the sequence.

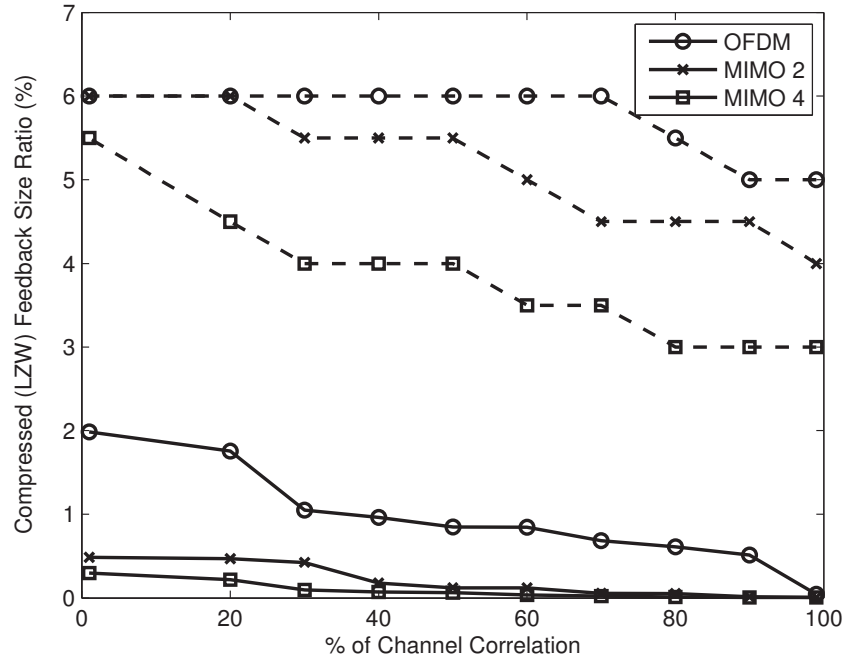


Figure 4.13. Compression of Feedback Size Ratio Achieved in OFDM and MIMO-OFDM Systems Using LZW Coding. Solid Lines for Compressed Feedback and Dotted Lines for Unreduced Feedback. Total Transmitted Bits = 5120000.

Finally, the LZW compression algorithm was applied to the reduced feedback obtained after applying the feedback reduction scheme to the systems. The Lempel-Ziv algorithm converts variable-length strings of input symbols into fixed length predictable codes. The symbol strings are selected so that all have almost equal probability of occurrence. Consequently, strings of frequently occurring symbols will contain more symbols than a string having infrequent symbols. So if there are a series of symbols repeating themselves very frequently in the feedback data, LZW can take advantage and achieve good compression ratios. Figure 4.13

shows the compression ratios achieved on the reduced feedback data in OFDM and MIMO-OFDM systems using LZW compression. Shown in the same figure in dotted lines is the uncompressed case to which the comparison has been done and compression ratios have been calculated. LZW coding, when applied to the reduced feedback data, achieved an average compression ratio of 83.8% in the OFDM system, 91.8% in MIMO 2×2 and 92.3% in MIMO 4×4 over all channel correlations. OFDM achieved a compression ratio of 98% for high channel correlation and 66% for no channel correlation. MIMO-OFDM 2×2 achieved a compression of 98% for high channel correlation and 84% for no channel correlation. MIMO-OFDM 4×4 achieved a compression of 98% for high channel correlation and 86% for no channel correlation. MIMO-OFDM 4×4 and MIMO-OFDM 2×2 achieved almost equal compression while outperforming OFDM by 9% more compression. From the results achieved we can see that LZW performed better than RLE compression and a little lower than Huffman coding. Huffman coding outperformed RLE and LZW in the OFDM system on average by 10% and 2%, and in MIMO-OFDM systems by 4% and 3%. When coming into high correlation channels, the compression ratios achieved by all three lossless compression algorithms remain the same. When the channel correlation was low, LZW could achieve higher compression than RLE, but less compression compared to Huffman coding. So, from all the results, we can say that assigning codes based on the probability of occurrence of symbols has proven to be the best compression possible in OFDM and MIMO-OFDM systems. When the channel correlation is high, any of the above compression algorithms would achieve significant compression, but when the channel correlation is low, the obvious choice of compression algorithm would be Huffman coding.

All the above simulations have been done to understand the performance of quantization levels with varying bits per sample. To understand the relation between different fixed quantization levels and the performance of OFDM and MIMO-OFDM systems and their compression ratios, all the above simulations have also been simulated with different quantization levels varying from 6 bits per sample to 1 bit per sample to be used for representing quantized energy allocation values. As explained, the total number of transmitted bits over all the 100 time-varying channel instances is constant and equal to 5120000 for all the cases. The results are shown below.

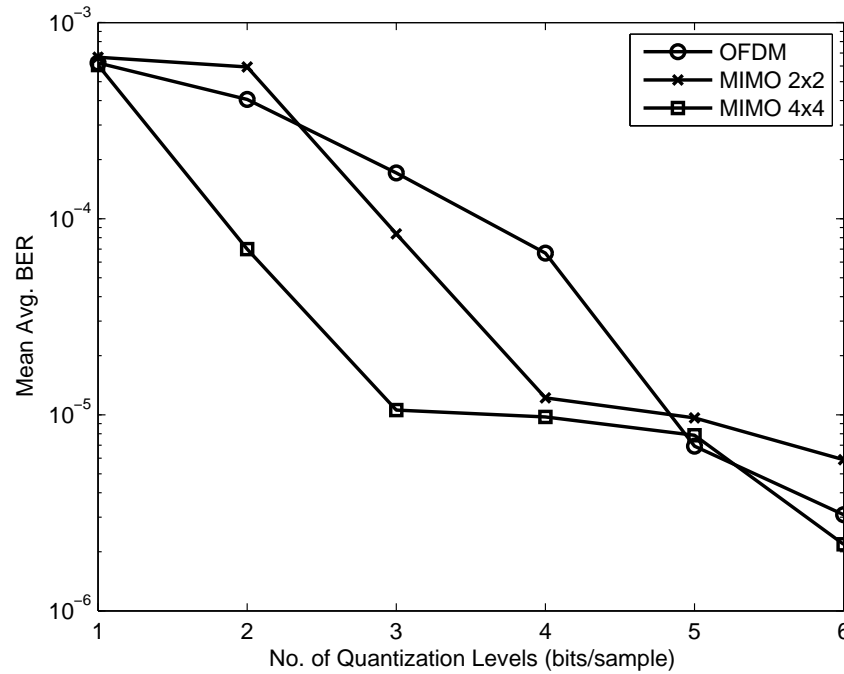


Figure 4.14. Mean of Average BER Curves for Various Energy Allocation Quantization Levels in OFDM and MIMO-OFDM Systems.

The performance of the system in terms of BER values as the quantization levels decreased is discussed here. Shown in Figure 4.14 is the relation between the mean average BER values achieved with varied energy allocation quantization

levels for various channel correlation values in OFDM and MIMO-OFDM systems. The x-axis values shown in the figure stand for the number of bits per sample used to represent quantization levels. Simulations have been done for bits per sample ranging from 6 to 1. As the quantization levels decreased, the BER values gradually increased in all the systems. As the quantization levels decrease, the quality of feedback is affected, and since this feedback is used for bit loading, it results in an increase in the error rate of the system. From the results, we can see that the advisable number of bits per sample to be used would be no less than 4 bits per sample, as below 4 bits per sample, the BER values of the system go beyond the threshold value and it would be a trade-off decision in choosing the number of quantization levels in terms of system performance. So, the performance of the OFDM and MIMO-OFDM systems in terms of BER values would meet the desired target if the number of bits per sample used were greater than 4 bits per sample.

The feedback reduction scheme has also been applied to systems employing various quantization levels. The feedback data size achieved for various quantization levels is discussed here. Figure 4.15 shows the effect of decreasing quantization levels on the data achieved using the feedback reduction scheme. As the bits per sample ranging from a maximum of 6 to a least value of 1 are used, the reduction ratios decreased for all the systems. As the quantization levels are decreased, due to bad feedback quality the system performance in terms of BER worsens. This in turn increases the number of feedback transmissions and so the size of feedback data. This leads finally, to a decrease in the feedback data size being achieved by the feedback reduction scheme. The OFDM system showed a decrease in the reduction ratio from 67% to 50%, whereas MIMO-OFDM 2×2 and MIMO-OFDM

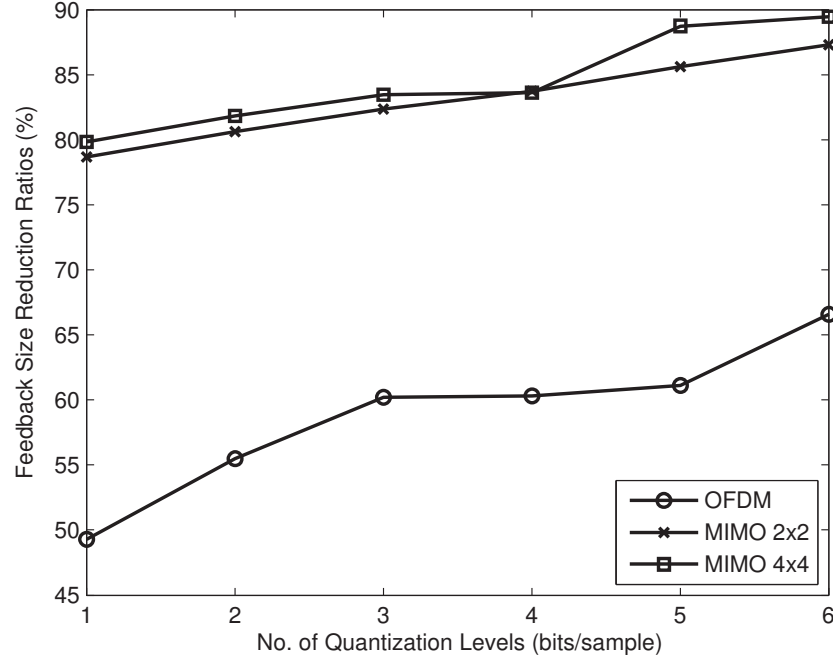


Figure 4.15. Reduction in Feedback Size Ratios Achieved Using Feedback Reduction Scheme for Various Energy Allocation Quantization Levels in OFDM and MIMO-OFDM Systems.

4×4 showed significantly less decrement from 87% and 89% to 79% and 80%. So, as the quantization levels decrease, the feedback reduction scheme becomes less efficient, especially in the OFDM case than in the MIMO-OFDM case. Since the quantization levels will be chosen based on the required BER target, if it would be more than 4 bits per sample it would still yield a reasonable reduction in the feedback data size.

As the quantization levels decrease, greater number of values fall into the same quantization levels, which in turn increases the repetition of the data, allowing the compression algorithms to achieve more and more compression. Shown are the compression ratios achieved when the compression algorithms discussed earlier were applied to the system employing various quantization levels. Figure 4.16

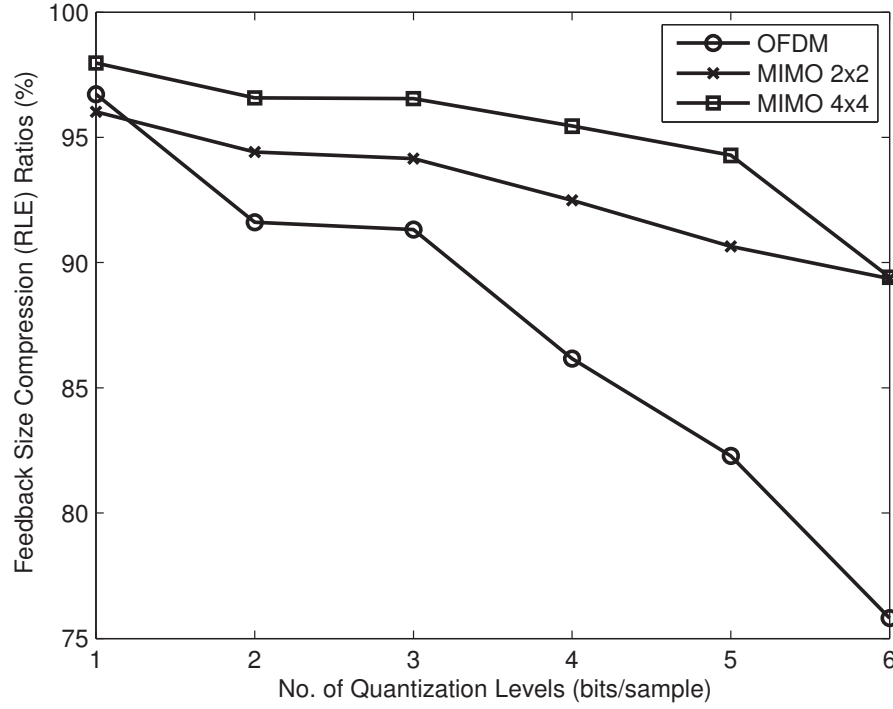


Figure 4.16. Compressed Feedback Size (RLE) Ratios for Various Energy Allocation Quantization Levels in OFDM and MIMO-OFDM Systems.

shows the compression ratios achieved in OFDM and MIMO-OFDM systems using RLE compression as quantization levels decrease. Once again OFDM shows the highest increase in the compression ratio as the quantization levels decrease beginning from 76% and continuing to 97%, whereas MIMO-OFDM 2×2 and MIMO-OFDM 4×4 start from 90% and rise to 95% and 98%. The MIMO-OFDM 4×4 system achieves the highest compression ratio in the case of RLE compression for least number of quantization levels used. There was a significant increase in the compression ratios when the number of quantization levels decreased.

Huffman coding outperformed the other algorithms when the number of quantization levels was 6 bits per sample. Shown here are the results of applying Huffman coding to the system with varying quantization levels. Figure 4.17 shows the

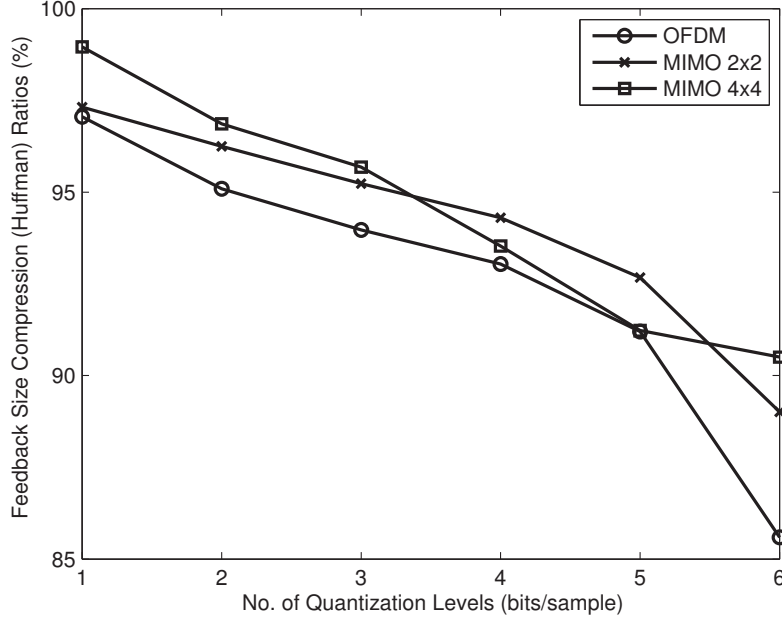


Figure 4.17. Compressed Feedback Size (Huffman) Ratios for Various Energy Allocation Quantization Levels in OFDM and MIMO-OFDM Systems.

compression ratios achieved in OFDM and OFDM-MIMO systems using Huffman compression as quantization levels decreased. Compression ratios in the OFDM system rose from 86% to 97% as the number of quantization levels decreased, whereas in MIMO-OFDM 2×2 it increased from 89% to 97% and in MIMO-OFDM 4×4 it increased from 92% to 98.5%. Huffman coding proves to be better than RLE again when the number of quantization levels decrease. The highest compression ratio achieved was for MIMO-OFDM 4×4 when the number of quantization levels were both highest and least. This demonstrates the efficiency of Huffman coding in compressing the feedback data of an adaptive multicarrier system.

LZW coding performed better than RLE and worse than Huffman in the case of fixed quantization levels. LZW performance, when the number of quantiza-

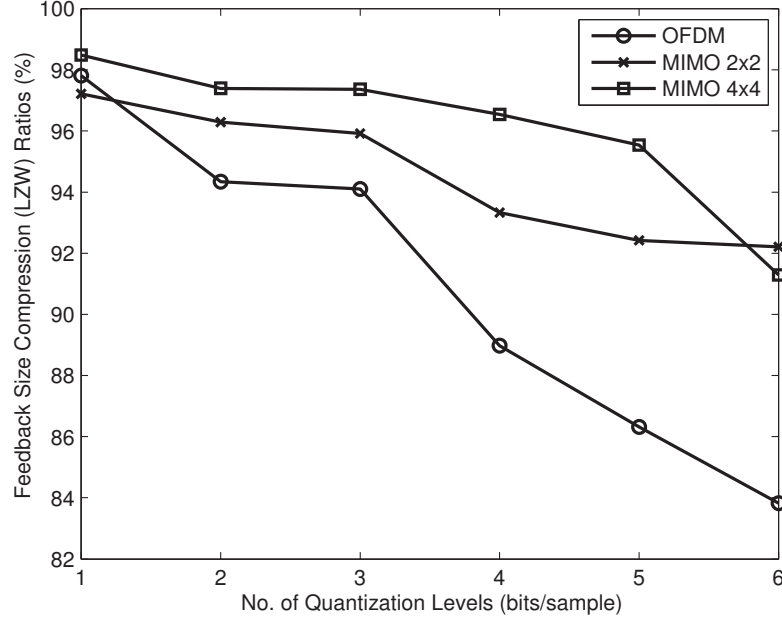


Figure 4.18. Compressed Feedback Size (LZW) Ratios for Various Energy Allocation Quantization Levels in OFDM and MIMO-OFDM Systems.

tion levels are varied is discussed here. Figure 4.18 shows the compression ratios achieved in OFDM and OFDM-MIMO systems using LZW compression as quantization levels decreased. Compression ratios in OFDM system rose from 84% to 97% as the number of quantization levels decreased, whereas in the MIMO-OFDM 2×2 they increased from 92% to 97% and in the MIMO-OFDM 4×4 they increased from 92% to 98.3%. The highest compression achieved by all three compression algorithms is almost equal where Huffman dominates with very minute differences. So, when the channel correlation is low and the number of quantization levels used in the system is also low, the best compression scheme would Huffman followed by LZW and the last option would be RLE. Additionally, the times of computation and urgency of requirement of results have to be taken into consideration when a compromise can be made on the compression ratios. If time frame is considered,

the best choice of compression algorithm that could be used will be Huffman followed by RLE and then, LZW. As explained earlier, even though better reduction and compression ratios can be achieved by using lower number of quantization levels, a trade-off has to be decided upon between the number of quantization levels and the required performance of the OFDM and MIMO-OFDM systems.

4.3 Chapter Summary

In this chapter, the descriptions of the simulation setup of the feedback reduction scheme and the method employed to compress the feedback data in adaptive multicarrier systems have been shown. By exploiting the time-correlation properties of the wireless channel, the feedback reduction scheme helped in reducing the number of feedback transmissions in adaptive systems and the existing lossless compression algorithms helped in compressing the feedback data. By using them jointly, the amount of feedback data has been significantly compressed.

According to the results, the feedback reduction scheme could achieve an average reduction of 60% for OFDM systems and 80% for MIMO-OFDM systems feedback data size. With the help of compression algorithms, Run Length Encoding, Huffman coding and LZW, an average compression ratio of 80% in OFDM systems and an average compression ratio of 90% in MIMO-OFDM systems has been achieved. Between, Huffman coding and LZW, although achieving very close compression ratios, Huffman has proven to be better than the remaining compression algorithms, and both Huffman and LZW outperformed RLE in all cases considered. Also, results have been shown to understand the relation between the different quantization levels and system performance. As the number of bits per sample decreased, the average BER of the system worsened, but there was

a increase in the compression ratio's. Thus, a trade-off has to be decided between the number of quantization levels and the required compression ratio based on the compromise to be made on requirements of the system performance. For our case, BER values meeting the threshold value would require no less than 4 bits per sample.

With the possibility of such significant compression of feedback data in adaptive multicarrier systems, these schemes are more suitable to be implemented in future mobile systems, increasing data throughput and overall system performance. The next chapter deals with the conclusions of this thesis and possible future work.

Chapter 5

Conclusions

In this thesis an attempt has been made to reduce the number of feedback transmissions and compress the feedback data being generated in wireless multicarrier transceivers using adaptive bit allocations. Consequently, we have been able to achieve a significant compression ratio. The achievements of this thesis are:

- OFDM concepts have been understood clearly and have been implemented through simulation; all interference removal techniques have been applied, creating an ideal system to be used for this work. The performance of the OFDM system has been measured while applying the time-varying channels with different correlations.
- The adaptive bit loading techniques have been researched and implemented on the OFDM system making it adaptive to the channel conditions. Analysis of the feedback data being generated in the adaptive OFDM system has been done and the need for compression of the feedback data has been clearly verified.

- Also, a clear understanding of the working of MIMO-OFDM systems has been obtained and implemented. The decomposition of the MIMO channel matrix into parallel channels using singular value decomposition, precoding and receiver shaping has been effectively implemented, so that the same bit loading algorithms can be applied to both OFDM and MIMO-OFDM systems.
- By doing a thorough literature survey, different lossless compression techniques suitable to be applied for compressing the feedback of adaptive systems have been confirmed and implemented.
- With the help of the feedback reduction scheme, the number of feedback transmissions in adaptive multicarrier transceiver systems has been reduced. This scheme exploits the time-correlation properties of the wireless channel and achieves an average reduction of 60% in the OFDM system and 80% in MIMO-OFDM systems feedback data size.
- A significant compression was achieved by applying source coding techniques such as RLE, Huffman coding and LZW on the reduced feedback data. Huffman coding outperformed the other two compression algorithms by achieving an average compression of 80% in the OFDM system and 90% in MIMO-OFDM systems. An understanding of the relationship between the number of quantization levels and the system performance and compression ratios possible have also been explained.

5.1 Future Work

These are a few areas of future work related to what has been presented in this thesis:

- Rigorous evaluation of the feedback reduction scheme in different system conditions would help us to understand its effectiveness and build a better and robust feedback reduction scheme.
- It would be interesting to see if the feedback reduction scheme could be implemented effectively on a cognitive radio.
- It would be nice to develop mathematical expressions for the error due to channel estimation and the error due to source coding, and both quantitatively evaluate and compare several techniques to determine suitable techniques for use with adaptive bit loading algorithms and the feedback compression.

References

- [1] Bingham, J. A. C., “Multicarrier modulation for data transmission: An idea whose time has come,” *IEEE Commun. Mag.*, vol. 5, pp. 5–14, March 1990.
- [2] R. Sacchi and P. Lorch, “Understanding the use of OFDM in IEEE 802.16 (WIMAX),” *Agilent Measurement J.*, vol. 2, pp. 8–13, 2007.
- [3] IEEE Std. 802.11a, “Wireless LAN medium access control (MAC) and physical layer (PHY) specifications: High-speed physical layer in the 5 GHz band,” Nov. 1999.
- [4] A. M. Wyglinski, *Physical layer loading algorithms for indoor wireless multicarrier systems*. Ph.d dissertation, McGill University, Montreal, Quebec, Canada, Nov. 2004.
- [5] G. L. Stuber, J. R. Barry, S. W. McLaughlin, Y. Li, M. Ingram, and T. Pratt, “Broadband MIMO-OFDM wireless communications,” *Proc. IEEE*, vol. 92, pp. 271–294, Feb. 2004.
- [6] A. M. Wyglinski and F. Labeau and P. Kabal, “An efficient bit allocation algorithm for multicarrier modulation,” in *Proc. IEEE Wireless Commun. Networking Conf.*, vol. 2, (Atlanta, GA, USA), pp. 1194–1199, Mar. 2004.

- [7] B. Fox, “Discrete optimization via marginal analysis,” *Management Science*, vol. 13, No. 3, pp. 210–216, Nov. 1966.
- [8] A. Leke and J. M. Cioffi, “A maximum rate loading algorithm for discrete multitone modulation systems,” in *Proc. IEEE Global Telecommun. Conf.*, vol. 3, (Phoenix, AZ, USA), pp. 1514–1518, Nov. 1997.
- [9] R. F. H. Fischer and J. B. Huber, “A new loading algorithm for discrete multitone transmission,” in *Proc. IEEE Global Telecommun. Conf.*, vol. 1, (London, UK), pp. 724–728, Nov. 1996.
- [10] A. Leke and J. M. Cioffi, “Impact of imperfect channel knowledge on the performance of multi-carrier systems,” in *Proc. IEEE Global Telecommun. Conf.*, vol. 2, (Sydney, Australia), pp. 951–955, Nov. 1998.
- [11] S. Ye, R. S. Blum, and L. J. Cimini, “Adaptive modulation for variable-rate OFDM systems with imperfect channel information,” in *Proc. 55th IEEE Veh. Technol. Conf. - Spring*, vol. 2, (Birmingham, AL, USA), pp. 767–771, May 2002.
- [12] M. R. Souryal and R. L. Pickholtz, “Adaptive modulation with imperfect channel information in OFDM,” in *Proc. IEEE Int. Conf. Commun.*, vol. 6, (Helsinki, Finland), pp. 1861–1865, June 2001.
- [13] H. Cheon and B. Park and D. Hong, “Adaptive multicarrier system with reduced feedback information in wideband radio channels,” in *Proc. 50th IEEE Veh. Technol. Conf. - Fall*, vol. 5, (Amsterdam, The Netherlands), pp. 2880–2884, Sept. 1999.

- [14] H. Nguyen and T. Lestable and V. Kumar and J. Brouet, “Adaptive multicarrier system with reduced feedback information in wideband radio channels,” in *Proc. 59th IEEE Veh. Technol. Conf. - Spring*, vol. 4, (Genoa, Italy), pp. 1916–1919, May 2004.
- [15] J. J. van de Beek, P. Ödling, S. K. Wilson and P. O. Börjesson, “Orthogonal frequency division multiplexing.” URSI, Wiley, 1999:2002.
- [16] J. G. Proakis and D. G. Manolakis, *Digital Signal Processing: Principles, Algorithms and Applications*. Macmillan, 1996.
- [17] A. Peled and A. Ruiz, “Frequency domain data transmission using reduced computational complexity algorithms,” *Proc. of the IEEE Intl. Conf. on Acoustics, Speech, and Signal Processing*, pp. 964–967, 1980.
- [18] A. Goldsmith, *Wireless Communications*. Cambridge University Press, 2005.
- [19] J. van de Beek, M. Sandell, and P. O. Börjesson, “ML estimation of time and frequency offset in OFDM systems,” *IEEE Trans. Signal Processing*, vol. 45, pp. 1800–1805, July 1997.
- [20] M. K. Simon, J. K. Omura, R. A. Scholtz, and B. K. Levitt, *Spread Spectrum Communications Handbook*. McGraw-Hill, 2001.
- [21] J. G. Proakis, *Digital Communications*. Prentice Hall,, 1995.
- [22] J. K. Cavers, “An analysis of pilot-symbol assisted modulation for rayleigh-fading channels,” *IEEE Trans. Veh. Technol.*, vol. 40, pp. 686–693, 1991.

- [23] A. V. Zelst and T. C. W. Schenk, "Implementation of a MIMO OFDM based wireless LAN system," *IEEE Trans. Signal Processing*, vol. 52, No. 2, Feb. 2004.
- [24] J. H. Sung and J. R. Barry, "Bit-allocation strategies for closed-loop MIMO OFDM," in *Proc. IEEE Veh. Technol. Conf.*, (Orlando, FL), 2003.
- [25] Y. Karasawa, "MIMO Propagation Channel Modeling," *IEICE Trans. Commun.*, vol. J86-B, No.9, pp. 1706–1720, Sept. 2003.
- [26] V. K. Madisetti and D. B. Williams, *The Digital Signal Processing Handbook*. CRC Press, 1998.
- [27] W. K. Tam and V. N. Tran, "Multi-ray propagation model for indoor wireless communications," *Electronics and Commun. Eng. J.*, vol. 32, pp. 135–137, 1996.
- [28] A. A. M. Saleh and R. A. Valenzuela, "A statistical model for indoor radio multipath propagation," *IEEE J. Select. Areas Commun.*, vol. 5, pp. 128–137, 1987.
- [29] T. S. Rappaport, *Wireless Communications, Principles and Practice*. New Jersey: Prentice-Hall, 1996.
- [30] M. C. Jeruchim, P. Balaban, and K. S. Shanmugan, *Simulation of Communication Systems*. New York: Plenum Press, 1992.
- [31] P. S. R. Diniz, E. A. B. D. Silva, and S. L. Netto, *Digital Signal Processing: System Analysis and Design*. Cambridge University Press, 2002.

- [32] K. S. Shanmugan, *Digital and Analog Communication Systems*. New York: John Wiley & Sons, 1985.
- [33] B. Farber and K. Zeger, "Optimality of the natural binary code for quantizers with channel optimized decoders," in *Proc. IEEE Int. Symp. Info Theory*, vol. 29, (Yokohoma, Japan), p. 483, 2003.
- [34] K. Sayood, *Introduction to Data Compression*. San Francisco: Morgan Kaufmann, 2000.
- [35] J. Ziv and A. Lempel, "Compression of Individual Sequences Via Variable-Rate Coding," *IEEE Tran on Information Theory*, vol. 24, pp. 530–536, 1978.
- [36] T. A. Welch, "A technique for high-performance data compression," *Computer*, vol. 17, pp. 8–19, 1984.
- [37] D. A. Huffman, "A method for the construction of minimum-redundancy codes," *Proc. IRE*, vol. 40, No. 9, pp. 1098–1101, Sep. 1952.
- [38] I. H. Witten and R. M. Neal and J. G. Cleary, "Arithmetic Coding for Data Compression," *Communications of the ACM*, vol. 30, pp. 520–540, 1987.
- [39] I. C. Wong and B. L. Evans, "Joint Channel Estimation and Prediction for OFDM systems," in *Proc. IEEE Global Telecom. Conf.*, vol. 4, (St. Louis, MO USA), pp. 2255–2259, 2005.
- [40] L. Hanzo, C. H. Wong, and M. S. Yee, *Adaptive Wireless Transceivers*. John Wiley & Sons, Ltd, 2002.
- [41] L. Hanzo, *OFDM and MC-CDMA for Broadband Multi-User Communications, WLANs and Broadcasting*. Wiley-IEEE Press, 2005.

- [42] T. Keller and L. Hanzo, "Blind-detection assisted sub-band adaptive turbo coded OFDM schemes," in *Proc. IEEE Veh. Technol. Conf.*, pp. 489–493, 1999.
- [43] B. S. Krongold, K. Ramchandran, and D. Jones, "Computationally Efficient Optimal Power Allocation Algorithms for Multicarrier Communication Systems," *IEEE Trans. Commun.*, vol. 48, pp. 23–27, 2000.
- [44] J. Campello, "Optimal discrete bit loading for multicarrier modulation system," in *Proc. IEEE Int. Symp. Info. Theory*, p. 193, 1998.
- [45] P. S. Chow, J. M. Cioffi, and J. A. C. Bingham, "A practical discrete multitone transceiver loading algorithm for data transmission over spectrally shaped channels," *IEEE Trans. Commun.*, vol. 43, pp. 773–775, 1995.
- [46] T. Lestable and M. Bartelli, "LZW Adaptive Bit Loading," in *Proc. IEEE Int. Symp. Advances Wireless Commun.*, (Victoria, Canada), Sep. 2002.
- [47] Y. Rong, S. A. Vorobyov, and A. B. Gershman, "On average one bit per sub-carrier channel state information feedback in ofdm wireless communication systems," in *Proc. IEEE Global Telecom. Conf.*, vol. 6, (Dallas, TX, USA), pp. 4011–4015, Dec. 2004.
- [48] Y. Teng, T. Nagaosa, K. Mori, and H. Kobayashi, "Proposal of grouping adaptive modulation method for burst mode ofdm transmission system," *IEICE Trans. Commun.*, vol. E86-B, No.1, pp. 257–265, Jan. 2003.
- [49] M. Lei and P. Zhang, "Subband bit and power loading for adaptive ofdm," in *Proc. 58th IEEE Veh. Technol. Conf.*, vol. 3, pp. 1482–1486, Oct. 2003.

- [50] G. Miao and Z. Niu, “Practical feedback design based ofdm link adaptive communications over frequency selective channels,” in *IEEE Int. Conf. Commun.*, vol. 10, (Istanbul, Turkey), pp. 4624–4629, June 2006.